2019-05-29

Kaposi Sarcoma-associated Herpesvirus Glycoprotein H is Indispensable for Infection of Epithelial, Endothelial, and Fibroblast Cell Types

Murali Muniraju
Beckman Research Institute of City of Hope

Et al.

Target Journals: JVI

Kaposi Sarcoma-associated Herpesvirus Glycoprotein H is Indispensable for Infection of Epithelial, Endothelial, and Fibroblast Cell Types

Murali Muniraju[a], Lorraine Z. Mutsvunguma[a], Joslyn Foley[a], Gabriela M. Escalante[a], Esther Rodriguez[a], Romina Nabiee[b], Jennifer Totonchy[b], David H. Mulama[a,c], Joshua Nyagol[a,d], Felix Wussow[a], Anne K. Barasa[a,d], Michael Brehm[e], and Javier Gordon Ogembo[a]#

[a]Department of Immuno-Oncology, Beckman Research Institute of City of Hope, Duarte, CA, USA

[b]Chapman University, School of Pharmacy, Irvine, CA, USA

[c]Biological Sciences Department, Masinde Muliro University of Science and Technology, Kakamega, Kenya

[d]Department of Human Pathology, University of Nairobi, Nairobi, Kenya

[e]Program in Molecular Medicine, University of Massachusetts Medical School, Worcester, MA, USA

Running Head: Glycoprotein H is Essential for Modulating KSHV Entry

#Address correspondence to Javier Gordon Ogembo, jogembo@coh.org

Abstract word count: 237

Text word count: 7,896

Keywords: Kaposi sarcoma-associated herpesvirus, glycoprotein H, mutation, viral entry, infection, tropism, epithelial, endothelial, fibroblast, B cell, cancer, vaccine.

Target Journals: JVI

ABSTRACT

Kaposi sarcoma-associated herpesvirus (KSHV) is an emerging pathogen and is the causative infectious agent of Kaposi sarcoma and two malignancies of B cell origin. To date, there is no licensed KSHV vaccine. Development of an effective vaccine against KSHV continues to be limited by a poor understanding of how the virus initiates acute primary infection *in vivo* in diverse human cell types. The role of glycoprotein H (gH) in herpesvirus entry mechanisms remains largely unresolved. To characterize the requirement for KSHV gH in the viral life cycle and in determination of cell tropism, we generated and characterized a mutant KSHV in which expression of gH was abrogated. Using a bacterial artificial chromosome containing a complete recombinant KSHV genome and recombinant DNA technology, we inserted stop codons into the gH coding region. We used electron microscopy to reveal that the gH-null mutant virus assembled and exited from cells normally, compared to wild-type virus. Using purified virions, we assessed infectivity of the gH-null mutant in diverse mammalian cell types *in vitro*. Unlike wild-type virus or a gH-containing revertant, the gH-null mutant was unable to infect any of the epithelial, endothelial, or fibroblast cell types tested. However, its ability to infect B cells was equivocal, and remains to be investigated *in vivo* due to generally poor infectivity *in vitro*. Together, these results suggest that gH is critical for KSHV infection of highly permissive cell types including epithelial, endothelial, and fibroblasts.

IMPORTANCE

All homologues of herpesvirus gH studied to date have been implicated in playing an essential role in viral infection of diverse permissive cell types. However, the role of gH in the mechanism of KSHV infection remains largely unresolved. In this study, we generated a gH-null mutant KSHV and provided evidence that deficiency of gH expression did not affect viral particle assembly or egress. Using the gH-null mutant, we showed that gH was indispensable for KSHV infection of epithelial, endothelial, and fibroblast cells *in vitro.*

47 This suggests that gH is an important target for the development of a KSHV prophylactic vaccine to prevent
48 initial viral infection.
49

Target Journals: JVI

INTRODUCTION

The oncogenic human Kaposi sarcoma-associated herpesvirus (KSHV), also known as human herpesvirus 8 (HHV-8), is a member of the γ-herpesvirus subfamily of the *Herpesviridae* family, which also includes Epstein-Barr virus (EBV) (1, 2). KSHV is the etiologic agent of Kaposi sarcoma (KS), the most common AIDS-associated cancer, as well as two malignancies of B cell origin, primary effusion lymphoma and multicentric Castleman disease (3, 4). KSHV can be transmitted via sexual contact, as well as through non-sexual routes, including contaminated blood transfusion, tissue transplant, or saliva contact, especially in children residing in endemic areas (5-10). KS is a major cause of morbidity and mortality in adults in sub-Saharan Africa, and is an emerging pediatric disease in children living with human immunodeficiency virus (11). The disease burden is exacerbated by a lack of preventive vaccines or effective KSHV-specific therapies to date. Although much research has focused on understanding the mechanism by which KSHV initiates primary infection and achieves broad tropism for diverse cell types [see reviews (12, 13)], the mechanisms defining KSHV cell tropism remain poorly characterized, due in part to a lack of animal models to test viral pathogenesis, and a limited spectrum of cultured cell lines that support lytic viral replication (14). This lack of knowledge continues to limit development of an effective vaccine against KSHV and its associated malignancies.

The genome of KSHV is 138,146 base pairs long (15, 16) and encodes for approximately 90 open reading frames (ORFs). It shows genetic homology to γ-1 EBV, γ-2 herpesvirus saimiri, and rhesus monkey rhadinovirus (1, 17, 18). Like other members of the *Herpesviridae* family, the large genome of KSHV encodes genes with diverse functions in distinct steps of the viral life cycle in host cells (19-21). *In vivo*, KSHV has been detected in B cells, epithelial cells, endothelial cells, fibroblasts, monocytes, and para-endothelial spindle cells (22, 23). *In vitro*, it broadly infects B cell, epithelial, endothelial, monocyte, and fibroblast cell lines of human and non-human origins (13, 24). KSHV enters permissive target cells through a multi-step process that involves

interactions between multiple viral envelope glycoproteins and host cell receptors that mediate viral attachment, fusion, entry, replication, assembly, egress, and even latency (25).

Cellular receptors and KSHV glycoproteins involved in viral infection have been well studied in various *in vitro* model infection systems. The KSHV envelope glycoproteins implicated in virus–cell attachment, fusion, and viral entry are ORF8 (gB), ORF22 (gH), ORF47 (gL), and K8.1. Both gB and K8.1 are thought to initiate viral entry through binding to host cell surface heparan sulfate proteoglycans on target cells to initiate infection in epithelial, endothelial, and fibroblast cell types (26-29). Similarly, some *in vitro* studies have implicated dendritic cell-specific adhesion molecule 3 (ICAM-3)-grabbing non-integrin (DC-SIGN) and cystine transporter xCT in viral entry (30, 31). Upon binding, conformational changes occur that are thought to allow the gH/gL complex to gain access to specific host cell receptors, including integrins and the erythropoietin-producing hepatocellular (Eph) receptors A2 (EphA2), EphA4, and EphA7 (32-34). Intriguingly, B cell lines have been reported to lack the ext1 enzyme that promotes glycosylation in heparan sulphate biosynthesis and were recently shown to lack expression of EphA2 (27, 35). This may explain why they are refractory to KSHV infection *in vitro* (25, 27, 28, 35, 36).

Working in concert with various non-conserved glycoproteins specific to each individual virus, the core conserved glycoproteins gB, gH, and gL, which are conserved among all herpesviruses, are thought to be necessary and sufficient for membrane attachment, fusion, and entry of all herpesviruses (37). In the current model of γ-herpesvirus entry, the virus attaches to host cell receptors through its non-conserved glycoproteins (e.g. gp350 or K8.1), which signals gH/gL to activate the gB fusogen. In this way, the gH/gL complex functions as an adaptor that transmits the triggering signal and activates viral fusion to the host cell membrane (37). However, the exact mechanisms behind these glycoprotein interactions, and how these interactions facilitate viral entry and modify viral tropism, remain poorly understood. Elucidating these mechanisms is challenging because the interactions are often transient and/or of low affinity. Unique among the core conserved proteins is the requirement for gH homologs to associate with gL and/or other proteins, depending on the type of

herpesvirus, in order to be correctly folded, transported within the infected cell, and incorporated into the viral envelope to ultimately modulate viral tropism (37). For instance, EBV gH forms a heterotrimeric complex with gL and gp42 (gH/gL-gp42), which subsequently enables binding of the N-terminal domain of gp42 to HLA class II to facilitate EBV infection of human B cells (38, 39). In contrast, the presence of gp42 inhibits EBV fusion and entry into epithelial cells (40-42). Although KSHV gH is known to form a heterodimeric complex with gL (gH/gL) via a non-covalent linkage in which the N-terminus of gH interacts with gL (26), whether KSHV gH/gL also complexes with additional envelope proteins remains unresolved. Importantly, the role of KSHV gH in viral maturation, assembly, egress, or infection remains undetermined. In addition, although several KSHV glycoprotein–host-cell receptor interactions have been described, it is not clear which viral envelope glycoproteins are essential for infection of most highly permissive cell types (31, 32, 43). Identification of the critical KSHV glycoproteins required for infection of permissive cells *in vivo* will provide information to guide prophylactic vaccine development.

As for all other herpesviruses, significant progress in studying KSHV gene functions has been made by deriving mutant viruses that harbor deletions, truncations, or insertions of stop codons within the gene of interest to abrogate protein expression via a bacterial artificial chromosome (BAC) system (44-51). Once the recombinant virus is constructed, the impact of the introduced mutations on the phenotypic properties of the virus can be determined using *in vitro* or *in vivo* systems. To date, only two KSHV deletion mutants (K8.1-null and gB-null) have been generated and partially characterized to understand the roles of envelope glycoproteins in entry mechanisms (44, 45). In this study, we generated and characterized a mutant KSHV virus in which expression of the gH protein was abrogated by insertion of stop codons into the gH coding region using *En Passant* mutagenesis, a two-step lambda Red DNA recombination system (52). To better define the role of gH in the KSHV life cycle, we assessed the ability of the gH-null mutant to replicate, produce virions, and infect diverse mammalian cell types *in vitro*. Using recombinant KSHV lacking gH protein, we provide evidence that KSHV gH is not required for virion maturation, assembly, or egress. Importantly, we show that gH is

indispensable for infection of epithelial, endothelial, or fibroblast cells of human origin *in vitro*, suggesting that KSHV gH is a key target for the development of a prophylactic vaccine to prevent KSHV entry and infection.

RESULTS

Mutagenesis, integrity analysis of genomic clones, and establishment of stable inducible cell lines. To determine the role of KSHV gH in cell entry, replication, and virus egress, we generated ORF22 (gH)-null recombinant KSHV tagged with enhanced green fluorescent protein (rKSHVΔgH-eGFP) and its revertant (rKSHVgH-eGFP Rev) based on wild-type eGFP-tagged recombinant KSHV (rKSHV WT-eGFP) within the E. coli strain GS1783. A sequence of three stop codons, TAGTTAGATAGT (a three-stop element that ensures protein translation machinery encounters a stop signal in all possible three reading frames), was inserted (ΔgH) or removed again after insertion (gH Rev) into the gH coding sequence of the rKSHV WT-eGFP genome using the two-step *En passant* markerless Red recombination system as described (15, 52). Because the gH gene overlaps with flanking sequences ORF21 and ORF23, the three-stop element was inserted downstream of the gH start codon at amino acid (aa) position 78 to avoid interference with the expression of the upstream ORF21 gene (**FIG. 1A**). During *En passant* mutagenesis, we confirmed insertion (step 1) and deletion (step 2) of a kanamycin resistance (Kan^R) gene cassette within the rKSHV WT-eGFP genome using PCR with flanking primers (ORF22-F and ORF22-R, listed in **Table 1**) (**FIG. 1B**) and restriction fragment length polymorphism analysis with HindIII restriction enzyme (**FIG. 1C**). We confirmed the sequence integrity of the mutation site in rKSHVΔgH-eGFP and rKSHVgH-eGFP Rev using Sanger sequencing (**FIG. 1D**). The complete genome sequence of rKSHVΔgH-eGFP following the mutagenesis procedure was identical to its parental rKSHV WT-eGFP clone, as confirmed using both Illumina Miseq and PacBio genome sequencing.

To obtain efficient and stable producer cell lines for rKSHVΔgH-eGFP or rKSHVgH-eGFP Rev, we used inducible SLK (iSLK) cells, a KSHV cell line containing a stable doxycycline (Dox)-inducible cassette of ORF50 (RTA) (15), a KSHV immediate-early gene that is necessary and sufficient for activating KSHV lytic replication. We transfected, selected, and characterized iSLK cells as described (15). Briefly, we transfected genomic DNAs of rKSHVΔgH-eGFP or rKSHVgH-eGFP Rev into iSLK cells, then selected transfected cells for hygromycin resistance (a gene located within the rKSHV-eGFP genome) until cells in the culture were all

stably eGFP-positive (**FIG. 2A**). Upon successful establishment of latency, we expanded the parental iSLK rKSHV WT-eGFP and stable iSLK rKSHVΔgH-eGFP and iSLK rKSHVgH-eGFP Rev cell lines, then treated them with Dox and sodium butyrate (NaB) to induce RTA expression. This led to the initiation of lytic gene expression and subsequent production of rKSHV WT-eGFP, rKSHVΔgH-eGFP, or rKSHVgH-eGFP Rev progeny virions, which we purified from the cell culture supernatants as described (15). We quantified the purified virions using qPCR and observed that induction of iSLK cells harboring the KSHV gH-null mutant or its revertant consistently released equal titers of virions compared to rKSHV WT-eGFP (**FIG. 2B**). We further confirmed the abrogation of gH expression in purified rKSHVΔgH-eGFP virions using immunoblot with an anti-gH monoclonal antibody (mAb) (clone 54A1, unpublished antibody generated in our laboratory) (**FIG. 2C**, top panel). In our hands, we found that gH expression is typically low in the KSHV-infected cells; thus, to detect gH protein in immunoblots, we used highly purified and concentrated samples of iSLK rKSHV WT-eGFP, rKSHVΔgH-eGFP, and rKSHVgH-eGFP Rev virions. We did not detect gH protein in lysates from purified rKSHVΔgH-eGFP virions, but did detect it in all three positive controls, i.e., lysates from purified rKSHV WT-eGFP and rKSHVgH-eGFP Rev virions and purified soluble gH/gL protein complex. As expected, we did not detect gH protein expression in lysates made from iSLK cells (negative control). To confirm that all three recombinant viruses were undergoing normal latent and lytic cycles, we demonstrated the presence of ORF73 (LANA1; a latent KSHV protein) and K8.1 (a lytic KSHV protein) in lysates from all recombinant cell types, but not iSLK negative control cells (**FIG. 2C**, middle and bottom panel).

gH is dispensable for production and egress of KSHV virions. To assess whether KSHV gH is critical for production or egress of virions from stable iSLK rKSHVΔgH-eGFP cells, we seeded equal amounts of iSLK rKSHV WT-eGFP, iSLK rKSHVΔgH-eGFP, or iSLK rKSHVgH-eGFP Rev cells and induced them with Dox and NaB for 48 h. To assess virion production, we washed and fixed the induced cells, prepared thin sections, and observed them using transmission electron microscopy (TEM), confirming that virions produced from

rKSHV WT-eGFP, rKSHVΔgH-eGFP, and rKSHVgH-eGFP Rev viruses were assembled within iSLK cells (**FIG. 3**, top panel). To assess egress, we filtered and concentrated the supernatant from the induced cells, then performed negative stain TEM, which confirmed that virions produced from all viruses were released into the supernatant (**FIG. 3**, bottom panel). These results indicate that KSHV gH is not required for maturation, assembly, or egress of the virus from iSLK cells.

KSHV gH is indispensable for cell-free viral infection of diverse highly permissive cell lines and primary fibroblasts. We used purified rKSHV WT-eGFP, rKSHVΔgH-eGFP, or rKSHVgH-eGFP Rev virions to determine infectivity and *in vitro* host range in various cell types. To assess infectivity in iSLK cells, we incubated cells with purified rKSHV WT-eGFP, rKSHVΔgH-eGFP, or rKSHVgH-eGFP Rev virions. Unlike iSLK cells incubated with rKSHV WT-eGFP or rKSHVgH-eGFP Rev, iSLK cells incubated with rKSHVΔgH-eGFP were not permissive to infection, even in the presence of infection enhancers such polybrene and/or spinoculation (**FIG. 4**).

To assess infectivity in other cell types permissive to KSHV infection (24, 53), we incubated iSLK cells (a mixture of endothelial and epithelial cells), human epithelial cell lines (HEK-293 and HeLa), human endothelial cells (HUVEC), and human fibroblasts (HFF-1 cell line and primary tonsil fibroblasts) with purified rKSHV WT-eGFP, rKSHVΔgH-eGFP, or rKSHVgH-eGFP Rev virions. As expected, rKSHV WT-eGFP and rKSHVgH-eGFP Rev infected all cell types tested, as determined using both flow cytometry and microscopy for eGFP expression (**FIG. 5A**). We obtained similar results in primary tonsil fibroblasts from four independent donors (**FIG. 5B**). In contrast, no infection was observed when any of these cell types were incubated with purified rKSHVΔgH-eGFP, indicating that gH protein is required for infectivity of these highly permissive cell types tested (**FIG. 5A–B**).

B cells typically exhibit poor permissiveness to KSHV infection *in vitro*, which is thought to be due to lack of appropriate receptors (54). Remarkably, when we infected a B cell line (MC116) with the purified

196 virions, then used flow cytometry to quantitate infection, we observed that rKSHV WT-eGFP, rKSHVΔgH-
197 eGFP, and rKSHVgH-eGFP Rev infected the cells (**FIG. 5C**), albeit to a limited extent. This suggests that gH is
198 not required for infection of this cell line or that KSHV can bypass the canonical receptors to cause infection of
199 MC116 cells. We used fluorescent microscopy to further confirm the infectivity of rKSHV WT-eGFP,
200 rKSHVΔgH-eGFP, and rKSHVgH-eGFP Rev for MC116 cells (**FIG. 5D**). Quantification of eGFP-positive
201 infected cells confirmed that infectivity of rKSHVΔgH-eGFP was comparable to that of rKSHV WT-eGFP and
202 rKSHVgH-eGFP Rev (**FIG. 5E,** top panel). Furthermore, when we used fluorescence-activated cell sorting
203 (FACS) to enrich for eGFP-positive cells, the resulting cells were able to multiply and spontaneously go lytic,
204 as evidenced by detection of the lytic protein, K8.1, by immunoblot (**FIG. 5E,** bottom panel). This suggests that
205 most MC116 infected cells are lytic in nature. We also detected expression of both LANA1 and K8.1 using real-
206 time quantitative PCR (RT-qPCR), which was comparable between rKSHV WT-eGFP- and rKSHVΔgH-eGFP-
207 infected cells (**FIG. 5F**).

208 To confirm that most of the human cell lines tested expressed the canonical cellular receptors that have
209 been implicated in supporting KSHV infection through gH/gL interactions, we analyzed expression of EphA2
210 and EphA4 using immunoblot, and expression of EphA7 using flow cytometry, due to lack of an antibody that
211 works for immunoblot. All of the cell types tested by immunoblotting expressed both EphA2 and EphA4
212 proteins, with the exception of MC116 cells, which only expressed EphA4 (**FIG. 5G**). This may explain the
213 limited permissiveness of MC116 cells to KSHV infection, as both EphA2 and EphA4 were recently shown to
214 synergistically support infection (32, 33). However, we detected expression of EphA7, which was recently
215 implicated in cell-cell transmission of KSHV infection, in MC116 cells but not in iSLK or HEK-293 cells (**FIG.**
216 **5H**). The role of EphA7 expression in permissiveness of MC116 cells to KSHV infection remains to be
217 investigated.

218 To confirm our infectivity data, we used non-human cell lines. We found that as for human cells, only
219 rKSHV WT-eGFP or rKSHVgH-eGFP Rev virions were infectious to epithelial (CHO-K1 and Vero) and

fibroblast (NIH 3T3 and BHK-21) cell lines (**FIG. 6**), whereas rKSHVΔgH-eGFP did not infect any of the non-human cell lines tested. Taken together, these results indicate that gH is required for KSHV infection of diverse non-B cell types.

gH is dispensable for KSHV binding to target cells. To measure the extent to which rKSHVΔgH-eGFP can bind to non-permissive cell lines, we performed viral binding/attachment assays. We incubated cells (HeLa, HUVEC, HFF-1, and MC116) with rKSHV WT-eGFP or rKSHVΔgH-eGFP at the indicated input concentrations (Log1–Log4 viral copies per cell, as quantified by qPCR), then washed them to remove unbound virus. We used qPCR to quantify total DNA isolated from cell-bound KSHV, viral genome copy number (using KSHV K8.1 gene), and the total number of cells (using GAPDH housekeeping gene), then plotted the ratio of viral DNA attached per cell against input viral genome copies per cell. We observed comparable target-cell attachment between rKSHV WT-eGFP and rKSHVΔgH-eGFP over a range of 4 log concentrations of input viral genome per cell in all cell types tested (**FIG. 7**). Comparable binding to epithelial cells, endothelial cells, fibroblast cells, and B cells indicates that the mutant virus retains its ability to bind multiple cell types, possibly using a non-gH/gL glycoprotein such as ORF4, K8.1, or gB. This suggests that although infection is abrogated by the absence of gH in epithelial, endothelial, and fibroblast cell types, the physical binding of rKSHVΔgH-eGFP to the cell surface is not affected in any cell types by the absence of gH.

Nucleotide sequence accession number. We deposited the full genome sequence of the rKSHVΔgH-eGFP construct (including BAC16, but excluding the inserted three-stop element) in GenBank under accession number MK208323.

DISCUSSION

KSHV is marked by a broad viral tropism for diverse host cell types, including epithelial and endothelial cells, fibroblasts, monocytes, and B cells [see reviews (12, 13)]. Like most herpesviruses, KSHV is shed in the saliva, suggesting it is principally transmitted via the oral epithelium (55-59). The virus then spreads to establish latency in other permissive cell types and remains in the host for life. However, a complete understanding of the KSHV life cycle remains elusive, and the KSHV glycoproteins mediating entry into and infection of diverse cell types remains unresolved. An improved understanding of these mechanisms is required to develop effective strategies for preventing KSHV infection and subsequent malignancies.

To gain an improved understanding of KSHV entry and infection mechanisms, we generated a stable iSLK rKSHVΔgH-eGFP producer cell line that enabled us to fully characterize the phenotype of rKSHV lacking gH expression. Upon lytic induction of iSLK rKSHVΔgH-eGFP cells, normal mature virus particles assembled and were released, indicating that gH is not required for KSHV maturation, assembly, or egress. Although our results contradict a recent observation that deletion of gH is deleterious to viral replication (60), we are confident in the results of our transmission electron microscopy studies, which showed that, as for most other herpesviruses, deletion of KSHV gH does not interfere with viral replication, maturation, or egress. Similar to an EBV gH-null mutant virus (39), we showed that rKSHV lacking gH expressed both latent (LANA1) and lytic (K8.1) genes, indicating that the viral replication cycle is not impaired. We further used the purified, functional, cell-free viral particles to define the role of gH in *de novo* infection and determine KSHV host range *in vitro*. Our results show that KSHV gH is indispensable for infection of human and non-human epithelial cells, endothelial cells, and fibroblasts; however, because we observed low efficiency of infection to the MC116 B cell line, we consider its role in human B cell infection to remain inconclusive. This is further confirmation that deletion of KSHV gH is not deleterious to viral replication.

In the past two decades, multiple host cell receptors in diverse permissive cell types have been identified as mediators of KSHV infection that interact with various KSHV glycoproteins such as K8.1, gB, and the gH/gL complex. These include integrins, heparan sulfate, cystine/glutamate transporter, DC-SIGN, and EphA2, A4, and A7 (26, 32, 61-65). Targeting host cell receptors offers one way to prevent KSHV infection. However, redundant functions among the receptors involved may hinder this approach. For example, although integrins such as α3β1, αVβ3 or αVβ5 are presumed to play a crucial role in KSHV infection (13), they were recently proven to be dispensable for epithelial cell infection (61), suggesting that they may not be ideal targets in a clinical setting. Similarly, a recent study identified conserved residues in the N-terminal domain of gH that mediate EphA2 binding (66). Mutation of the residues reduced infection efficiency in iSLK cells, but did not completely block KSHV infection, prompting the authors to conclude that gH binding to EphA2 is important but not essential for viral infection, suggesting that either multiple sites on gH interact with EphA2 or other host receptors are likely involved in the infection. Indeed, in another study, single or combined knockout of EphA2 and EphA4 in HEK-293 cells dramatically decreased KSHV infection, but did not achieve complete blockage of infection (33), as we achieved in our current experiments in which lack of gH expression completely blocked KSHV infection of diverse cell types. Additional evidence shows that targeting individual host cell receptors is not an effective mechanism for blocking KSHV infection, as neither knocking out cellular receptors (61, 67) nor using inhibitors to target cellular receptors, including peptides, small molecules, or soluble receptors, has completely inhibited KSHV infection in diverse permissive cell types [reviewed in (12)]. Furthermore, potential challenges in targeting host cell receptors clinically to prevent KSHV infection include: (1) the high quantities of blocking reagents required for systemic distribution may prove toxic; (2) the expression levels of host cell receptors may be transient and/or depend upon the cell state (e.g., activated vs. inactivated B cells show differential DC-SIGN expression); (3) the necessity of using multiple blocking reagents to target the multiple types of receptors expressed on permissive host cells; and (4) the potential for different receptors to bind to different sites of the same KSHV glycoprotein(s) mediating infection.

To counter the challenges inherent in targeting host cell receptors to prevent KSHV infection, we suggest that targeting multiple viral glycoproteins involved in viral entry may be more effective. Our study provides strong evidence that expression of KSHV gH is absolutely required for infection of epithelial cells, endothelial cells, and fibroblasts. Although KSHV lacking gH was capable of binding to these cell types, it did not infect them, even at high viral DNA copy number. Coupled with published data on EphA2/A4 knockout, this suggests that the gH/gL complex interacts with more than two host cell receptors engaged in viral infection in epithelial, endothelial, and fibroblast cells (35). Recent isolation of broadly neutralizing mAbs against other herpesviruses such as EBV gH/gL (AMMO1) (68), or human cytomegalovirus gH/gL pentameric complex (69), suggests that such antibodies may exist for KSHV and that KSHV gH/gL may be useful targets for developing prophylactic vaccines to elicit broadly neutralizing antibodies to prevent infection in epithelial, endothelial, and fibroblast cells.

Despite remarkable progress made in elucidating general γ-herpesvirus entry mechanisms into highly permissive cell types, how KSHV enters B cells both *in vitro* and *in vivo* remains unresolved. In striking contrast to the abrogated infection we observed in epithelial cells, endothelial cells, and fibroblasts, and to its closest related human γ-herpesvirus, EBV (39), our gH-null KSHV mutant infected a well-characterized permissive B cell line (MC116) *in vitro* to a limited extent. This infection was characterized by lytic induction, as evidenced by readily detectable K8.1 protein without artificial induction of lytic replication using chemical reagents. Given our preliminary observations that gH-null virus was infectious to B cells, we speculate that KSHV entry into B cells likely occurs through another envelope glycoprotein, K8.1, and its binding to a yet-to-be determined receptor, as was recently reported (54). The importance of K8.1 for B cell infection was recently demonstrated by Dollery at el; their group showed that blocking K8.1 with mAbs or a K8.1-null mutant rKSHVΔK8.1 (45, 70) significantly reduced KSHV infection of a B cell line (MC116) and tonsillar primary B cells, but not epithelial or endothelial cell lines. However, whether this infection occurs in the absence of gH remains to be investigated. It is also possible that KSHV enters and infects B cells through a direct interaction

between gB and DC-SIGN or EphA4 (30), or a yet-to-be identified receptor, bypassing gH and K8.1 altogether. However, elucidating the role of KSHV gB in infection is not straightforward. Using a BAC system, a previous study demonstrated that KSHV gB-null mutant virus can replicate, but that its virions neither mature nor egress outside of host cells to release infectious particles, making it difficult to test the ability of rKSHV lacking gB protein to infect cells (44). Thus, future studies could explore the use of a protease-sensitive gB mutant or gB-neutralizing antibodies as an alternative strategy to elucidate the role(s) of gB in viral entry and identify its receptor in B cells. However, to our knowledge, there are currently no such reagents available to fully characterize the phenotype of a KSHV gB-null mutant virus. Regarding B cell entry via gH/gL, our findings and current cumulative evidence suggest that the gH/gL–EphA2 interaction does not play any role in the infection of B cells, given that EphA2 is not expressed on most B cells (26, 66, 71). However, our results showed for the first time that MC116 cells express both EphA4 and EphA7, both of which have been implicated in KSHV infection, either through cell-free viral infection or cell-to-cell transmission (33, 34). These receptors may provide a mechanism for KSHV entry and infection of B cells or other cell types; however, their roles remain to be elucidated.

In summary, this work highlights the utility of the BAC system and Red recombination technique in dissecting the functional role of KSHV gH protein in viral replication and *de novo* infection of a variety of target cells. We provide evidence that KSHV gH is not required for viral maturation, virion assembly, or egress, and that it is indispensable for infection of epithelial cells, endothelial cells, and fibroblast cells. Thus, we suggest that gH is a key target for the development of prophylactic vaccines to prevent initial KSHV infection. However, the role of gH in B cell infection remains inconclusive, and we will continue to investigate this role in our laboratory in a humanized BLT (bone marrow, liver, and thymus) mouse model generated from NOD/SCID/IL2rγ mice, which have been shown to be susceptible to KSHV infection and to develop KSHV-positive B cell lymphoma (72). We expect results from the present and future studies to fully inform

development of an effective subunit vaccine or a promising antiviral target against KSHV infection and its associated malignancies.

MATERIALS AND METHODS

Viruses and cells. We received 1) the iSLK cell line containing stable Dox-inducible RTA, and 2) iSLK cells harboring recombinant WT KSHV (rKSHV WT-eGFP; GenBank accession number GQ994935.1) as kind gifts from Dr. Jung, University of Southern California, CA. rKSHV WT-eGFP contains the viral clone JSC-1 previously isolated from primary effusion lymphoma cells in a BAC 16 backbone incorporating eGFP and hygromycin resistance as selection markers in its genome (15). Human embryonic kidney epithelial cells (HEK-293), human cervical epithelial cells (HeLa), human umbilical vein endothelial cells (HUVEC), human foreskin fibroblasts (HFF-1), human EBV- and KSHV-negative lymphoblastoid B cell line (MC116), Chinese hamster ovary epithelial-like cells (CHO-K1), African green monkey endothelial cells (Vero), mouse fibroblast cells (NIH/3T3), and Syrian golden baby hamster kidney fibroblasts (BHK-21) were obtained from American Type Culture Collection (ATCC, Manassas, VA). These cells were maintained as recommended by ATCC either in Dulbecco's modified Eagle's medium (DMEM) or Roswell Park Memorial Institute (RPMI) 1640 media with 2 mM L-glutamine, 10% fetal bovine serum (FBS), and 1% penicillin/streptomycin antibiotics. HUVEC were maintained in VascuLife Basal Medium with VascuLife EnGS LifeFactors (Lifeline Cell Technology, Frederick, MD). iSLK cells were cultured with 2 mM L-glutamine, 10% FBS, and 1% penicillin/streptomycin antibiotics in DMEM medium supplemented with 1 µg/ml puromycin and 250 µg/ml G418. All cell lines were cultured at 37°C in a humidified, 5% CO_2 incubator.

De-identified primary human tonsil fibroblasts were obtained after routine tonsillectomy from discarded, de-identified tissues, with approval from the Institutional Review Board of Chapman University. Non-lymphocyte tonsil lineages were isolated via homogenization of residual tonsil tissue after lymphocyte extraction by incubating the tissue with 1120 units Liberase DH (5401054001; Roche, Indianapolis, IN) and

200 µg DNaseI (DN25; Sigma Aldrich, St. Louis, MO) in serum-free DMEM for 2 x 15 min at 37˚C, with homogenization between and after incubations using a Miltenyi gentleMACS instrument (Miltenyi Biotec, San Diego, CA). The resulting single-cell suspensions were cultured as mixed lineage, high-density cultures in endothelial cell media containing 100 µg/ml antimicrobial Primocin (InvivoGen, San Diego, CA) for 7-10 days to facilitate adaptation to 2-dimensional cell culture. Fibroblasts were then isolated from adapted cultures using positive selection via magnetic microbeads (CD90 microbeads 130-096-253; Miltenyi). After isolation, primary CD90+ fibroblasts were maintained in DMEM containing 10% FBS and Primocin, and were used for experiments between passage 3 and 10.

Plasmids and mutagenesis of KSHV WT-eGFP genome. To generate plasmid for qPCR standardization, full-length WT K8.1 was individually cloned into the pCAGGS mammalian expression vector as described (73). To construct gH/gL Fc-6xHis-tagged plasmids for protein production, a single transcript expressing WT gL (gL-WT; aa 1-139) and the gH ectodomain (aa 1-702) was synthesized by Genewiz (South Plainfield, NJ). The upstream (5') and downstream (3') sequences contained NotI and SpeI enzyme restriction sites, respectively (74), which were used to subclone the synthesized product into the Cntn1-Fc-His vector, a gift from Dr. Wojtowicz, Stanford University, CA (Addgene plasmid #72065). To express gH/gL complex in its native form, a unique 2A linker sequence (18 aa) (75) was interspersed between the cDNAs encoding for the two proteins. This resulted in a polycistronic vector with a cleavage site that allows gL-WT and the gH ectodomain to be processed independently after transcription, and released to natively form a complex that is released into the supernatant. Sanger sequencing was used to verify the fidelity of the whole vector and the construct.

pEPkan-S plasmid was used as a source of the Kan^R gene cassette required for *En Passant* mutagenesis (12). rKSHV WT-eGFP within the E. coli strain GS1783 was a kind gift of Dr. Jung (15). rKSHV WT-eGFP was used as a vector in which three stop codons (TAGTTAGATAGT) were introduced within ORF22 (gH) at nucleotide position 37,165 using *En Passant* mutagenesis, a two-step, markerless Red recombination technique,

as described (15, 52). This resulted in a truncated sequence devoid of gH protein expression. The cloning mutagenesis strategy and the primers used for insertion (to make rKSHVΔgH-eGFP) and removal (to make rKSHVgH-eGFP Rev) of the three-stop element are illustrated in **FIG. 1A** and **Table 1**. Recombinant clones with insertion or deletion of the Kan^R cassette in the rKSHV WT-eGFP genome following the two-step Red recombination technique were digested with HindIII, and the site of mutation was PCR-amplified using primers flanking the region and analyzed by agarose-gel electrophoresis. The mutated sites of each rKSHV WT-eGFP clone and the integrity of the whole genome were confirmed using Sanger sequencing and next-generation sequencing, respectively.

Whole genome sequencing and sequence analysis. Genome sequencing of the purified rKSHVΔgH-eGFP DNA from GS1783 bacteria was performed using standard protocols, as described (15). To confirm the integrity of the genome, approximately 2 µg of rKSHVΔgH-eGFP genomic DNA was fragmented using the Covaris S220 Ultrasonicator System (Matthew, NC), and sheared DNA size was assessed using the Agilent 2011 bioanalyzer (Santa Clara, CA). A SMRTbell library was constructed following the PacBio standard 20-kb template preparation protocol using the SMRTbell Template Prep Kit 1.0 from Pacific Biosciences (Menlo Park, CA). Briefly, the DNA was incubated with exonuclease VII at 37°C for 15 min to remove single-stranded DNA, and any possible DNA damage was repaired using a DNA damage repair mix at 37°C for 20 min. Blunt-ended DNAs were treated with end-repair mix at 25°C for 5 min and ligated with 1 µM of annealed blunt adapters using 0.75 U/µl ligase at 25°C overnight, then the ligase was inactivated by incubation at 65°C for 10 min. To remove failed ligation products, samples were treated with exonuclease III and VII at 37°C for 1 h. To purify the DNAs and ligated products, 0.45X of AMPure PB Beads from Pacific Biosciences were applied. The final magbead complexes were loaded into a PacBio RSII machine for SMRT sequencing, with one SMRT cell allocated to the complex for 6 h running time.

Primary whole genome sequencing analysis, including real-time imaging, base calling, and assessing quality was performed by the PacBio RS Blade Center through RS Touch and RS Remote, and the results were sent directly to secondary analysis for extracting the filtered subreads with SMRT Pipe (v.1.87.139483) via SMRT Portal (v.2.3.0). The filtered 445,558 subreads were used as the input for the Canu sequence assembler (v.1.7.1) (76) for *de novo* assembly, and the assembled sequence from Canu was corrected using LoRDEC (v.0.9) (77), based on Illumina short reads obtained from the same DNA sample generated using an Illumina MiSeq.

Production and quantification of recombinant KSHV progeny. Purified rKSHVΔgH-eGFP and rKSHVgH-eGFP Rev DNAs were introduced into iSLK cells using FuGENE® HD transfection reagent (Promega, Madison, WI) (12). Transfected cells were selected in media containing hygromycin at a final concentration of 1 mg/ml, which was also used to maintain stable iSLK cell lines harboring latent KSHV. To produce the progeny virus, these stable cell lines were expanded into 100 T-175 flasks, induced by addition of 2 µg/ml Dox and 1.5 mM of NaB to the culture media, and incubated for 24 h, after which the induction media was removed and cells were cultured in complete DMEM for four days as described (15). Progeny virus particles in the harvested cell culture supernatant were clarified twice by centrifugation at 2,000 ×g for 15 min, followed by filtration through a 0.8 µm membrane to remove cellular debris. Virions were pelleted by ultra-centrifugation (10,000 ×g for 90 min at 4°C) through a 5% Optiprep (Sigma Aldrich) gradient, and resuspended in 1x phosphate buffered saline (PBS) or media without FBS for subsequent experiments.

Viral titers were measured in iSLK Infectious Units (iSLU), assessed using either flow cytometry with eGFP expression as a marker for virus-positive cells, or quantitative PCR (qPCR) of genomic DNA copy number in virus stock. Briefly, for eGFP, serial dilutions of the viral preparations were used to infect iSLK cells; 24 h post-infection, the number of live cells expressing eGFP was determined using a fixable viability dye eFluor 506 and C-6 flow cytometer (BD Biosciences, San Jose, CA) and data was analyzed using FlowJo

Cytometry Analysis software (FlowJo, LLC, Ashland, OR). For qPCR, DNA was extracted from the virus stock (pre-treated with DNase) using a QIAamp Mini Elute Virus Spin Kit (Qiagen, Valencia, CA). Viral genomes were quantified using PowerUp SYBR green PCR master mix or Taqman Fast Advanced Master Mix (Applied Biosystems, Foster City, CA) utilizing the primer pair ORF11/K8.1 or Taqman primers and probes targeting the BAC16 eGFP cassette. Samples were analyzed in triplicate. An eight-series of 10-fold dilutions of plasmid pCAGGS-K8.1 (73) or pCR2.1-GFP was used as a standard for absolute quantification of viral genome copies. The sequences of reverse transcriptase qPCR primer sets for amplification of viral ORF targets are provided in **Table 1**.

Transmission electron microscopy. Cells were trypsinized, washed with 1x PBS, and pelleted before fixing with 2% glutaraldehyde in 0.1 M Cacodylate buffer ($Na(CH_3)_2AsO_2 \cdot 3H_2O$), pH 7.2, at 4°C, overnight. Fixed cell pellets were washed three times with 0.1 M Cacodylate buffer, pH 7.2, post-fixed with 1% OsO_4 in 0.1 M Cacodylate buffer for 30 min, and washed three times with 0.1 M Cacodylate buffer. The samples were then dehydrated through 60%, 70%, 80%, and 95% ethanol, 100% absolute ethanol (twice), and propylene oxide (twice), and were left in propylene oxide/Eponate (1:1) overnight at room temperature (RT) in sealed vials. The next day, the vials were left open for 2–3 h to evaporate the propylene oxide. The samples were infiltrated with 100% Eponate and polymerized at 64°C for 48 h. Ultra-thin sections (~70 nm thick) were cut using a Leica Ultracut UCT ultramicrotome (Wetzlar, Germany) with a diamond knife and picked up on 200-mesh copper TEM grids. Grids were stained with 2% uranyl acetate for 10 min, followed by Reynold's lead citrate staining for 1 min. To perform negative stain TEM of extracellular progeny virus particles, the harvested supernatant was clarified by centrifugation at 2,000 ×g for 15 min, followed by filtration through 0.8 µm membrane to remove cellular debris. Purified virions were pelleted using ultra-centrifugation through a 5% Optiprep gradient at 10,000 ×g, 70 min, 4°C, then fixed in 2% glutaraldehyde and processed for TEM. Briefly, individual purified virions were resuspended in 1x PBS and solution was adsorbed to glow-discharged, carbon-coated 300 mesh

TEM grids. Samples were prepared using conventional negative staining with 1% (w/v) uranyl acetate. TEM images for both cells and purified virions were collected with an FEI Tecnai 12 transmission electron microscope (Thermo Fisher Scientific) equipped with a LaB6 filament and operated at an acceleration voltage of 120 kV. Images were recorded with a Gatan 2×2 k CCD camera (Gatan, Inc., Pleasanton, CA) at a magnification of 30,000X and a defocus value of ~1.5 µm.

Immunoblot. Cells were washed three times with 1x PBS, lysed with radio immunoprecipitation assay (RIPA) buffer, and centrifuged at 20,000 ×g for 10 min at 4°C. Total protein was quantified using Bradford protein assay (Thermo Fisher Scientific). Cleared total cellular lysate was mixed with reducing SDS loading buffer (125 mM Tris-HCl, 2% sodium dodecyl sulfate, 0.1% bromophenol blue, 1% 2-mercaptoethanol) at a ratio of 1:4, denatured at 100°C for 5 min, and separated using SDS-PAGE (NuPAGE™ 4-12% Bis-Tris Protein gel, Thermo Fisher Scientific). Separated proteins were transferred onto 0.45-µm nitrocellulose membranes (Protran; PerkinElmer Life Sciences, Waltham, MA). Membranes were then blocked with 3% BSA in 0.1% Tween 20 1x PBS for 1 h and probed with an appropriate primary antibody (in-house anti-gH mouse mAb, mab-54A1; anti-HHV-8 K8.1 A/B 4A4 mouse mAb [Santa Cruz Biotechnology, Dallas, TX]; anti-HHV-8 LNA-1 Clone LN53 rat mAb [Millipore, Burlington, MA]; anti-EphA2 (C-3; sc-398832) mouse mAb [Santa Cruz Biotechnology]; EphA4 (D4; sc-365503) mouse mAb [Santa Cruz Biotechnology]; or anti-β-actin (C-3; sc-47778) [Santa Cruz Biotechnology]) in blocking solution overnight at 4°C. The next day, membranes were washed three times (1x PBS and 0.1% Tween 20) and incubated with the corresponding horseradish peroxidase (HRP)-conjugated secondary antibodies (goat anti-mouse or goat anti-rat serum [Santa Cruz Biotechnology] at a dilution of 1:2,000) for 1 h at RT. After a subsequent wash, signal was developed using standard Amersham ECL Prime Western Blotting Detection reagent (GE Healthcare Life Sciences, Marlborough, MA) and the images were captured using an iBright Imaging System (Thermo Fisher Scientific).

***In vitro* infection assay.** $5x10^4$ cells/well (iSLK, HEK-293, HeLa, HUVEC, HFF-1, MC116, CHO-K1, Vero, NIH3T3, BHK-21, or primary human fibroblasts) were seeded ($5x10^4$/well) in 48-well plates in triplicate. The following day, cells were incubated with varying quantities (10^2 to 10^4 viral copies per cell) of purified rKSHV WT-eGFP (positive control), rKSHVΔgH-eGFP, or rKSHVgH-eGFP Rev in 1 ml of Opti-MEM media. Cells incubated in media without any virus were used as negative controls. The virus–cell mixtures were incubated at 37°C in 5% CO_2 for 2 h, then cells were washed three times with 1x PBS to remove unbound virus. Infected cells were incubated with complete media for 48 h and quantified by counting eGFP expression using flow cytometry. In certain cases, 8 µg/ml of polybrene was added to the infection media and/or spinoculation was performed by centrifugation at 1,500 ×g, for 1 h at RT, to enhance iSLK, primary fibroblast and B cell infections. All infection experiments were replicated at least three times and repeated twice.

Gene expression analysis in B cells. Cultured B cells (MC116) were infected and cultured as described above. Mock viral infection was performed using purified rKSHV WT-eGFP inactivated in 2% buffered formaldehyde in PBS for 60 min at 37°C. Infected cells were FACS-sorted (BD FACSAria III) and enriched for eGFP expression. Sorted cells were grown for 4 days, then harvested, pelleted, and lysed in 300 µl TRIzol reagent and stored at -80°C until analysis. After thawing, 300 µl of DNA/RNAShield reagent (Zymo Research R1100-50) were added to the TRIzol and RNA was isolated using a Zymo Directzol RNA miniprep kit (Zymo Research R2050). An additional DNase step was performed after RNA extraction using a Turbo DNA-free kit (Thermo Fisher Scientific AM1907). RNA yield was quantitated using a Qubit fluorimeter and 100 ng of total RNA was used for cDNA synthesis in a 20-µl reaction using a High-Capacity cDNA Reverse Transcription Kit (Thermo Fisher Scientific 4368814). Additional control reactions for each infected condition were performed without reverse transcriptase enzyme to verify the efficiency of DNA removal from the samples. Three µl of the resulting cDNA was used in triplicate wells for RT-qPCR analysis. Primers for RT-qPCR are listed in **Table 1**.

Ct values from replicate wells were averaged and copy number of individual gene expression was quantified using rKSHV WT-eGFP DNA.

Quantification of viral binding/attachment using qPCR. To define the mechanistic role of gH in virion attachment to cell surface receptors, binding/attachment assays were performed to analyze rKSHV WT-eGFP and rKSHVΔgH-eGFP binding to target cell lines *in vitro* as described (66). Briefly, $2x10^5$ cells/well of HeLa, HUVEC, HFF-1, or MC116 cell types were seeded in 12-well plates overnight. The following day, target cells were incubated with ice-cold virus dilutions at the indicated concentrations (normalized to 10^2 to 10^4 genome copy numbers per cell as measured above by qPCR) at 4°C for 30 min. Cells were washed three times with ice-cold PBS to remove unbound virus, then bound virus was quantified using qPCR. Samples were analyzed in triplicate and repeated three times. Briefly, genomic DNA was isolated from cell-bound KSHV using the QIAamp Mini Elute Virus Spin Kit. The ratio of viral DNA to cellular DNA as a measurement of attached virus was determined by qPCR as described above (**FIG. 7**). The relative values of bound viral copy number to cellular DNA were calculated on the basis of cycle threshold (ΔCt) values for viral genomic loci (K8.1) and a cellular genomic locus (GAPDH).

Statistics. Data on viral titers are summarized as means ± SD. P-values were calculated using Kruskal-Wallis nonparametric test for the difference between means, comparing each experimental group with the control group. For all analyses, P-values of less than 0.05 are considered statistically significant. P-values (N.S.: not significant, $P < 0.05$, $P < 0.001$) are shown in each figure.

ACKNOWLEDGEMENTS

This work was supported by the National Institutes of Health (NIH) K01 CA184388-02 to JGO. Research reported in this publication included work performed in City of Hope Core Facilities including Analytical

Target Journals: JVI

Cytometry, Electron Microscopy, Integrative Genomics and Bioinformatics, Small Animal Studies, Drug Discovery & Structural Biology, and Pathology Research Services supported by the National Cancer Institute of the NIH under award number P30CA033572. The content is solely the responsibility of the authors and does not necessarily represent the official views of the National Institutes of Health. The funding agencies had no role in study design, data collection and data analysis, preparation of the manuscript, or decision to publish. We thank Dr. Jae Jung and Dr. Woj Wojtowicz for generous gifts of research materials. We thank Ms. Supriya Bautista for her help with the organization of figures and Dr. Sarah T. Wilkinson for editing the manuscript and offering insightful feedback and discussion.

REFERENCES

1. **Arias C, Weisburd B, Stern-Ginossar N, Mercier A, Madrid AS, Bellare P, Holdorf M, Weissman JS, Ganem D.** 2014. KSHV 2.0: A Comprehensive Annotation of the Kaposi's Sarcoma-Associated Herpesvirus Genome Using Next-Generation Sequencing Reveals Novel Genomic and Functional Features. PLOS Pathogens **10:**e1003847.
2. **Wen KW, Damania B.** 2010. Kaposi Sarcoma-associated Herpesvirus (KSHV): Molecular Biology and Oncogenesis. Cancer letters **289:**140-150.
3. **Ablashi DV, Chatlynne LG, Whitman JE, Cesarman E.** 2002. Spectrum of Kaposi's Sarcoma-Associated Herpesvirus, or Human Herpesvirus 8, Diseases. Clinical Microbiology Reviews **15:**439-464.
4. **Sullivan RJ, Pantanowitz L, Casper C, Stebbing J, Dezube BJ.** 2008. HIV/AIDS: epidemiology, pathophysiology, and treatment of Kaposi sarcoma-associated herpesvirus disease: Kaposi sarcoma, primary effusion lymphoma, and multicentric Castleman disease. Clin Infect Dis **47:**1209-1215.
5. **Minhas V, Wood C.** 2014. Epidemiology and Transmission of Kaposi's Sarcoma-Associated Herpesvirus. Viruses **6:**4178-4194.
6. **Biryahwaho B, Dollard SC, Pfeiffer RM, Shebl FM, Munuo S, Amin MM, Hladik W, Parsons R, Mbulaiteye SM.** 2010. Sex and geographic patterns of human herpesvirus 8 infection in a nationally representative population-based sample in Uganda. J Infect Dis **202:**1347-1353.
7. **Plancoulaine S, Abel L, van Beveren M, Tregouet DA, Joubert M, Tortevoye P, de The G, Gessain A.** 2000. Human herpesvirus 8 transmission from mother to child and between siblings in an endemic population. Lancet **356:**1062-1065.
8. **Caterino-de-Araujo A, Cibella SE.** 2003. Searching for antibodies to HHV-8 in children born to HIV-1 infected mothers from Sao Paulo, Brazil: relationship to maternal infection. J Trop Pediatr **49:**247-250.
9. **Brayfield BP, Kankasa C, West JT, Muyanga J, Bhat G, Klaskala W, Mitchell CD, Wood C.** 2004. Distribution of Kaposi sarcoma-associated herpesvirus/human herpesvirus 8 in maternal saliva and breast milk in Zambia: implications for transmission. J Infect Dis **189:**2260-2270.

10. **Chagas CA, Endo LH, Sakano E, Pinto GA, Brousset P, Vassallo J.** 2006. Detection of herpesvirus type 8 (HHV8) in children's tonsils and adenoids by immunohistochemistry and in situ hybridization. Int J Pediatr Otorhinolaryngol **70:**65-72.
11. **Haller JO.** 1997. AIDS-related malignancies in pediatrics. Radiol Clin North Am **35:**1517-1538.
12. **Chandran B.** 2010. Early events in Kaposi's sarcoma-associated herpesvirus infection of target cells. J Virol **84:**2188-2199.
13. **Veettil MV, Bandyopadhyay C, Dutta D, Chandran B.** 2014. Interaction of KSHV with host cell surface receptors and cell entry. Viruses **6:**4024-4046.
14. **Kaleeba JA, Berger EA.** 2006. Broad target cell selectivity of Kaposi's sarcoma-associated herpesvirus glycoprotein-mediated cell fusion and virion entry. Virology **354:**7-14.
15. **Brulois KF, Chang H, Lee AS, Ensser A, Wong LY, Toth Z, Lee SH, Lee HR, Myoung J, Ganem D, Oh TK, Kim JF, Gao SJ, Jung JU.** 2012. Construction and manipulation of a new Kaposi's sarcoma-associated herpesvirus bacterial artificial chromosome clone. J Virol **86:**9708-9720.
16. **Purushothaman P, Dabral P, Gupta N, Sarkar R, Verma SC.** 2016. KSHV Genome Replication and Maintenance. Frontiers in Microbiology **7:**54.
17. **Neipel F, Albrecht JC, Fleckenstein B.** 1997. Cell-homologous genes in the Kaposi's sarcoma-associated rhadinovirus human herpesvirus 8: determinants of its pathogenicity? Journal of Virology **71:**4187-4192.
18. **Searles RP, Bergquam EP, Axthelm MK, Wong SW.** 1999. Sequence and genomic analysis of a Rhesus macaque rhadinovirus with similarity to Kaposi's sarcoma-associated herpesvirus/human herpesvirus 8. J Virol **73:**3040-3053.
19. **Bruce AG, Ryan JT, Thomas MJ, Peng X, Grundhoff A, Tsai CC, Rose TM.** 2013. Next-generation sequence analysis of the genome of RFHVMn, the macaque homolog of Kaposi's sarcoma (KS)-associated herpesvirus, from a KS-like tumor of a pig-tailed macaque. J Virol **87:**13676-13693.
20. **Chang Y, Cesarman E, Pessin MS, Lee F, Culpepper J, Knowles DM, Moore PS.** 1994. Identification of herpesvirus-like DNA sequences in AIDS-associated Kaposi's sarcoma. Science **266:**1865-1869.
21. **Olp LN, Jeanniard A, Marimo C, West JT, Wood C.** 2015. Whole-Genome Sequencing of Kaposi's Sarcoma-Associated Herpesvirus from Zambian Kaposi's Sarcoma Biopsy Specimens Reveals Unique Viral Diversity. J Virol **89:**12299-12308.
22. **Boshoff C, Schulz TF, Kennedy MM, Graham AK, Fisher C, Thomas A, McGee JO, Weiss RA, O'Leary JJ.** 1995. Kaposi's sarcoma-associated herpesvirus infects endothelial and spindle cells. Nat Med **1:**1274-1278.
23. **Dupin N, Fisher C, Kellam P, Ariad S, Tulliez M, Franck N, van Marck E, Salmon D, Gorin I, Escande JP, Weiss RA, Alitalo K, Boshoff C.** 1999. Distribution of human herpesvirus-8 latently infected cells in Kaposi's sarcoma, multicentric Castleman's disease, and primary effusion lymphoma. Proc Natl Acad Sci U S A **96:**4546-4551.
24. **Bechtel J. T LY, Hvidding J, Ganem D.** 2003. Host range of Kaposi's sarcoma-associated herpesvirus in cultured cells. J Virol **77:**6474-6481.
25. **Dyson OF, Traylen CM, Akula SM.** 2010. Cell Membrane-bound Kaposi's Sarcoma-associated Herpesvirus-encoded Glycoprotein B Promotes Virus Latency by Regulating Expression of Cellular Egr-1. The Journal of Biological Chemistry **285:**37491-37502.
26. **Hahn A, Birkmann A, Wies E, Dorer D, Mahr K, Sturzl M, Titgemeyer F, Neipel F.** 2009. Kaposi's sarcoma-associated herpesvirus gH/gL: glycoprotein export and interaction with cellular receptors. J Virol **83:**396-407.
27. **Jarousse N, Chandran B, Coscoy L.** 2008. Lack of heparan sulfate expression in B-cell lines: implications for Kaposi's sarcoma-associated herpesvirus and murine gammaherpesvirus 68 infections. J Virol **82:**12591-12597.

28. **Akula SM, Pramod NP, Wang FZ, Chandran B.** 2001. Human herpesvirus 8 envelope-associated glycoprotein B interacts with heparan sulfate-like moieties. Virology **284:**235-249.
29. **Luna RE, Zhou F, Baghian A, Chouljenko V, Forghani B, Gao SJ, Kousoulas KG.** 2004. Kaposi's sarcoma-associated herpesvirus glycoprotein K8.1 is dispensable for virus entry. J Virol **78:**6389-6398.
30. **Rappocciolo G, Hensler HR, Jais M, Reinhart TA, Pegu A, Jenkins FJ, Rinaldo CR.** 2008. Human herpesvirus 8 infects and replicates in primary cultures of activated B lymphocytes through DC-SIGN. J Virol **82:**4793-4806.
31. **Kaleeba JA, Berger EA.** 2006. Kaposi's sarcoma-associated herpesvirus fusion-entry receptor: cystine transporter xCT. Science **311:**1921-1924.
32. **Hahn AS, Kaufmann JK, Wies E, Naschberger E, Panteleev-Ivlev J, Schmidt K, Holzer A, Schmidt M, Chen J, Konig S, Ensser A, Myoung J, Brockmeyer NH, Sturzl M, Fleckenstein B, Neipel F.** 2012. The ephrin receptor tyrosine kinase A2 is a cellular receptor for Kaposi's sarcoma-associated herpesvirus. Nat Med **18:**961-966.
33. **Chen J, Zhang X, Schaller S, Jardetzky TS, Longnecker R.** 2019. Ephrin Receptor A4 is a New Kaposi's Sarcoma-Associated Herpesvirus Virus Entry Receptor. MBio **10**.
34. **Großkopf AK, Schlagowski S, Hörnich BF, Fricke T, Desrosiers RC, Hahn AS.** 2019. EphA7 functions as a receptor for cell-to-cell transmission of Kaposi's sarcoma-associated herpesvirus into BJAB B cells and for cell-free virus infection by the related rhesus monkey rhadinovirus. bioRxiv**:**522243.
35. **Chen J, Sathiyamoorthy K, Zhang X, Schaller S, Perez White BE, Jardetzky TS, Longnecker R.** 2018. Ephrin receptor A2 is a functional entry receptor for Epstein-Barr virus. Nat Microbiol **3:**172-180.
36. **Birkmann A, Mahr K, Ensser A, Yağuboğlu S, Titgemeyer F, Fleckenstein B, Neipel F.** 2001. Cell Surface Heparan Sulfate Is a Receptor for Human Herpesvirus 8 and Interacts with Envelope Glycoprotein K8.1. Journal of Virology **75:**11583-11593.
37. **Connolly SA, Jackson JO, Jardetzky TS, Longnecker R.** 2011. Fusing structure and function: a structural view of the herpesvirus entry machinery: A structural view of herpesvirus entry machinery. Nat Rev Microbiol **9:**369-381.
38. **Sathiyamoorthy K, Hu YX, Mohl BS, Chen J, Longnecker R, Jardetzky TS.** 2016. Structural basis for Epstein-Barr virus host cell tropism mediated by gp42 and gHgL entry glycoproteins. Nat Commun **7:**13557.
39. **Molesworth SJ, Lake CM, Borza CM, Turk SM, Hutt-Fletcher LM.** 2000. Epstein-Barr virus gH is essential for penetration of B cells but also plays a role in attachment of virus to epithelial cells. Journal of virology **74:**6324-6332.
40. **Kirschner AN, Lowrey AS, Longnecker R, Jardetzky TS.** 2007. Binding-site interactions between Epstein-Barr virus fusion proteins gp42 and gH/gL reveal a peptide that inhibits both epithelial and B-cell membrane fusion. J Virol **81:**9216-9229.
41. **Kirschner AN, Omerovic J, Popov B, Longnecker R, Jardetzky TS.** 2006. Soluble Epstein-Barr virus glycoproteins gH, gL, and gp42 form a 1:1:1 stable complex that acts like soluble gp42 in B-cell fusion but not in epithelial cell fusion. J Virol **80:**9444-9454.
42. **Liu F, Marquardt G, Kirschner AN, Longnecker R, Jardetzky TS.** 2010. Mapping the N-terminal residues of Epstein-Barr virus gp42 that bind gH/gL by using fluorescence polarization and cell-based fusion assays. J Virol **84:**10375-10385.
43. **Cancian L, Hansen A, Boshoff C.** 2013. Cellular origin of Kaposi's sarcoma and Kaposi's sarcoma-associated herpesvirus-induced cell reprogramming. Trends Cell Biol **23:**421-432.
44. **Krishnan HH, Sharma-Walia N, Zeng L, Gao SJ, Chandran B.** 2005. Envelope glycoprotein gB of Kaposi's sarcoma-associated herpesvirus is essential for egress from infected cells. J Virol **79:**10952-10967.

45. **Luna R. E ZF, Baghlan A, Chouljenko V, Forghani B, Gao S. J and Kousoulas K. G.** 2004. Kaposi's sarcoma-associated herpesvirus glycoprotein K8.1 is dispensable for virus entry. J Virol **78:**6389-6398.
46. **Nishimura M, Watanabe T, Yagi S, Yamanaka T, Fujimuro M.** 2017. Kaposi's sarcoma-associated herpesvirus ORF34 is essential for late gene expression and virus production. Sci Rep **7:**329.
47. **Zhang Z, Chen W, Sanders MK, Brulois KF, Dittmer DP, Damania B.** 2016. The K1 Protein of Kaposi's Sarcoma-Associated Herpesvirus Augments Viral Lytic Replication. J Virol **90:**7657-7666.
48. **Brulois K, Toth Z, Wong LY, Feng P, Gao SJ, Ensser A, Jung JU.** 2014. Kaposi's sarcoma-associated herpesvirus K3 and K5 ubiquitin E3 ligases have stage-specific immune evasion roles during lytic replication. J Virol **88:**9335-9349.
49. **Gelgor A, Kalt I, Bergson S, Brulois KF, Jung JU, Sarid R.** 2015. Viral Bcl-2 Encoded by the Kaposi's Sarcoma-Associated Herpesvirus Is Vital for Virus Reactivation. J Virol **89:**5298-5307.
50. **Wang X, Zhu N, Li W, Zhu F, Wang Y, Yuan Y.** 2015. Mono-ubiquitylated ORF45 Mediates Association of KSHV Particles with Internal Lipid Rafts for Viral Assembly and Egress. PLoS Pathog **11:**e1005332.
51. **Wang F, Guo Y, Li W, Lu C, Yan Q.** 2018. Generation of a KSHV K13 deletion mutant for vFLIP function study. J Med Virol **90:**753-760.
52. **Tischer BK, Smith GA, Osterrieder N.** 2010. En passant mutagenesis: a two step markerless red recombination system. Methods Mol Biol **634:**421-430.
53. **Dollery SJ, Santiago-Crespo RJ, Kardava L, Moir S, Berger EA.** 2014. Efficient infection of a human B cell line with cell-free Kaposi's sarcoma-associated herpesvirus. J Virol **88:**1748-1757.
54. **Dollery SJ, Santiago-Crespo RJ, Chatterjee D, Berger EA.** 2018. Glycoprotein K8. 1A of Kaposi's sarcoma-associated herpesvirus is a critical B cell tropism determinant, independent of its heparan sulfate binding activity. Journal of Virology**:**JVI. 01876-01818.
55. **Jones T, Ye F, Bedolla R, Huang Y, Meng J, Qian L, Pan H, Zhou F, Moody R, Wagner B, Arar M, Gao SJ.** 2012. Direct and efficient cellular transformation of primary rat mesenchymal precursor cells by KSHV. J Clin Invest **122:**1076-1081.
56. **Matthews NC, Goodier MR, Robey RC, Bower M, Gotch FM.** 2011. Killing of Kaposi's sarcoma-associated herpesvirus-infected fibroblasts during latent infection by activated natural killer cells. Eur J Immunol **41:**1958-1968.
57. **Mutlu AD, Cavallin LE, Vincent L, Chiozzini C, Eroles P, Duran EM, Asgari Z, Hooper AT, La Perle KM, Hilsher C, Gao SJ, Dittmer DP, Rafii S, Mesri EA.** 2007. In vivo-restricted and reversible malignancy induced by human herpesvirus-8 KSHV: a cell and animal model of virally induced Kaposi's sarcoma. Cancer Cell **11:**245-258.
58. **Parsons CH, Adang LA, Overdevest J, O'Connor CM, Taylor JR, Jr., Camerini D, Kedes DH.** 2006. KSHV targets multiple leukocyte lineages during long-term productive infection in NOD/SCID mice. J Clin Invest **116:**1963-1973.
59. **Wu W, Vieira J, Fiore N, Banerjee P, Sieburg M, Rochford R, Harrington W, Jr., Feuer G.** 2006. KSHV/HHV-8 infection of human hematopoietic progenitor (CD34+) cells: persistence of infection during hematopoiesis in vitro and in vivo. Blood **108:**141-151.
60. **TerBush AA.** 2018. Characterization of receptor use and entry mechanisms in two KSHV infection systemsUC Berkeley.
61. **TerBush AA, Hafkamp F, Lee HJ, Coscoy L.** 2018. A Kaposi's Sarcoma-Associated Herpesvirus Infection Mechanism Is Independent of Integrins alpha3beta1, alphaVbeta3, and alphaVbeta5. J Virol **92**.
62. **Akula SM, Pramod NP, Wang F-Z, Chandran B.** 2001. Human herpesvirus 8 envelope-associated glycoprotein B interacts with heparan sulfate-like moieties. Virology **284:**235-249.

63. **Akula SM, Pramod NP, Wang FZ, Chandran B.** 2002. Integrin alpha3beta1 (CD 49c/29) is a cellular receptor for Kaposi's sarcoma-associated herpesvirus (KSHV/HHV-8) entry into the target cells. Cell **108:**407-419.
64. **Akula SM, Wang FZ, Vieira J, Chandran B.** 2001. Human herpesvirus 8 interaction with target cells involves heparan sulfate. Virology **282:**245-255.
65. **Birkmann A, Mahr K, Ensser A, Yağuboğlu S, Titgemeyer F, Fleckenstein B, Neipel F.** 2001. Cell surface heparan sulfate is a receptor for human herpesvirus 8 and interacts with envelope glycoprotein K8. 1. Journal of virology **75:**11583-11593.
66. **Grosskopf AK, Ensser A, Neipel F, Jungnickl D, Schlagowski S, Desrosiers RC, Hahn AS.** 2018. A conserved Eph family receptor-binding motif on the gH/gL complex of Kaposi's sarcoma-associated herpesvirus and rhesus monkey rhadinovirus. PLoS Pathog **14:**e1006912.
67. **Lisabeth EM, Falivelli G, Pasquale EB.** 2013. Eph receptor signaling and ephrins. Cold Spring Harb Perspect Biol **5**.
68. **Snijder J, Ortego MS, Weidle C, Stuart AB, Gray MD, McElrath MJ, Pancera M, Veesler D, McGuire AT.** 2018. An antibody targeting the fusion machinery neutralizes dual-tropic infection and defines a site of vulnerability on Epstein-Barr virus. Immunity **48:**799-811. e799.
69. **Ha S, Li F, Troutman MC, Freed DC, Tang A, Loughney JW, Wang D, Wang I-M, Vlasak J, Nickle DC.** 2017. Neutralization of diverse human cytomegalovirus strains conferred by antibodies targeting viral gH/gL/pUL128-131 pentameric complex. Journal of virology **91:**e02033-02016.
70. **Zhu L, Puri V, Chandran B.** 1999. Characterization of human herpesvirus-8 K8.1A/B glycoproteins by monoclonal antibodies. Virology **262:**237-249.
71. **Zhang H, Li Y, Wang HB, Zhang A, Chen ML, Fang ZX, Dong XD, Li SB, Du Y, Xiong D, He JY, Li MZ, Liu YM, Zhou AJ, Zhong Q, Zeng YX, Kieff E, Zhang Z, Gewurz BE, Zhao B, Zeng MS.** 2018. Ephrin receptor A2 is an epithelial cell receptor for Epstein-Barr virus entry. Nat Microbiol **3:**1-8.
72. **McHugh D, Caduff N, Barros MHM, Ramer PC, Raykova A, Murer A, Landtwing V, Quast I, Styles CT, Spohn M, Fowotade A, Delecluse HJ, Papoudou-Bai A, Lee YM, Kim JM, Middeldorp J, Schulz TF, Cesarman E, Zbinden A, Capaul R, White RE, Allday MJ, Niedobitek G, Blackbourn DJ, Grundhoff A, Munz C.** 2017. Persistent KSHV Infection Increases EBV-Associated Tumor Formation In Vivo via Enhanced EBV Lytic Gene Expression. Cell Host Microbe **22:**61-73 e67.
73. **Barasa A, Ye P, Phelps M, Ganapathiram A, Tison T, Ogembo JG.** 2017. BALB/c mice immunized with a combination of virus-like particles incorporating Kaposi sarcomaassociated herpesvirus (KSHV) envelope glycoproteins gpK8.1, gB, and gH/gL induced comparable serum neutralizing antibody activity to UV-inactivated KSHV Oncotarget **8:**34481-34497.
74. **Gibson DG, Young L, Chuang RY, Venter JC, Hutchison CA, 3rd, Smith HO.** 2009. Enzymatic assembly of DNA molecules up to several hundred kilobases. Nat Methods **6:**343-345.
75. **Kim JH, Lee SR, Li LH, Park HJ, Park JH, Lee KY, Kim MK, Shin BA, Choi SY.** 2011. High cleavage efficiency of a 2A peptide derived from porcine teschovirus-1 in human cell lines, zebrafish and mice. PLoS One **6:**e18556.
76. **Koren S, Walenz BP, Berlin K, Miller JR, Bergman NH, Phillippy AM.** 2017. Canu: scalable and accurate long-read assembly via adaptive k-mer weighting and repeat separation. Genome Res **27:**722-736.
77. **Salmela L, Rivals E.** 2014. LoRDEC: accurate and efficient long read error correction. Bioinformatics **30:**3506-3514.

Target Journals: JVI

Figure Legends and Tables

FIG. 1. Mutagenesis of rKSHVΔgH-eGFP. (a) Schematic showing construction of gH-null BAC clone (rKSHVΔgH-eGFP) and its revertant (rKSHVgH-eGFP Rev). Using an *En Passant* two-step Red recombination system, three stop codons were inserted into the gH (ORF22) coding region of rKSHV WT-eGFP (nt37166–nt37167; accession number GQ994935.1) to construct rKSHVΔgH-eGFP and subsequently removed to obtain rKSHVgH-eGFP Rev. **(b)** Agarose-gel electrophoresis of rKSHV-eGFP amplified using gene-specific primers flanking the mutation region shows integration and removal of kanamycin-resistance cassette (Kan^R) in the indicated BAC clones during the two-step *En Passant* red recombination technique. The amplicon size indicates insertion (~ 2.1 Kb) and deletion (~ 1.1 Kb) of a kanamycin-resistance cassette in each BAC clone. **(c)** Agarose-gel electrophoresis of rKSHV BACmids, digested with HindIII. The arrowheads indicate the variation in the length of restriction fragments due to insertion and deletion of Kan^R in the indicated BAC clones. **(d)** DNA sequencing results of gH mutagenesis sites show the sequence of the three-stop codon insertion site in the gH (nt37165) coding regions of full-length rKSHV WT-eGFP, rKSHVΔgH-eGFP, and rKSHVgH-eGFP Rev.

FIG. 2. Establishment and characterization of stable iSLK cell lines expressing rKSHVΔgH-eGFP and its revertant. (a) eGFP expression in iSLK cells stably transfected with KSHV genome. Purified rKSHVΔgH-eGFP or rKSHVgH-eGFP Rev DNA from bacteria were transfected into iSLK cells to generate stable virus producer cell lines, and stable iSLK cell lines expressing latent rKSHVΔgH-eGFP or rKSHVgH-eGFP Rev were selected. iSLK cells were used as a negative control; iSLK cells expressing rKSHV WT-eGFP were used as a positive control. Cells were imaged for eGFP expression using an EVOS Cell Imaging System at identical settings under 10x magnification. **(b)** qPCR quantification of KSHV genome copies. Equal numbers of seeded cells (iSLK rKSHV WT-eGFP, iSLK rKSHVΔgH-eGFP, or iSLK rKSHVgH-eGFP Rev) were induced into a lytic cycle; the virus produced was purified and genome copy number was quantified using qPCR with KSHV K8.1 primers (top panel), as compared to the absolute quantification standard curve obtained using pCAGGS-

K8.1 (bottom panel). P-values were calculated using a Kruskal-Wallis nonparametric test, and showed there was no difference in viral titers. **(c)** To assess expression of gH, LANA1, and K8.1 proteins, iSLK stable cells (negative control), iSLK rKSHV WT-eGFP (positive control), iSLK rKSHVΔgH-eGFP, or iSLK rKSHVgH-eGFP Rev were induced for lytic replication. Purified virions from iSLK rKSHV WT-eGFP, iSLK rKSHVΔgH-eGFP, iSLK rKSHVgH-eGFP Rev, purified gH/gL protein (for anti-gH detection), or induced infected cells (for LANA1 and K8.1 protein detection) were lysed and separated on 4-12% SDS-PAGE gels, and analyzed by immunoblotting using specific monoclonal antibodies against gH/gL (top), LANA1 (middle), or K8.1 (bottom).

FIG. 3. rKSHVΔgH-eGFP matures, assembles, and egresses into the supernatant, as shown by electron microscopy (TEM) of cultured cells and purified viruses. iSLK rKSHV WT-eGFP, iSLK rKSHΔgH-eGFP, and iSLK rKSHVgH-eGFP Rev cells were lytically induced for 96 h, virions released into the supernatant were purified, and cells and supernatant/virions were processed for TEM. Briefly, cells were collected, washed in PBS, and fixed in 2% glutaraldehyde. Thin sections were made and observed using TEM. Representative TEM images (n=3 experiments) of ultra-thin sections of cultured cells with internalized virions (upper row) or TEM images of negatively stained purified virions (bottom row) are provided.

FIG. 4. Infection of iSLK cells with rKSHVΔgH-eGFP. iSLK cells seeded ($5x10^4$/well) in 48-well plates were incubated with purified virus obtained from induced iSLK rKSHV WT-eGFP, iSLK rKSHVΔgH-eGFP, or iSLK rKSHVgH-eGFP Rev cells (equal amount diluted in 0.5 ml of Opti-MEM media +/- 8 µg/ml of polybrene as indicated), then spinoculated (as indicated) by centrifuge at 1,500 ×g for 1 h at 30°C. Complete media was added and plates were incubated for 48 h at RT, then observed using EVOS Cell Imaging fluorescent microscopy for eGFP expression. Images are representative pictures of experiments repeated in triplicate with 10^2 to 10^4 viral genome copies per cell.

FIG. 5. rKSHVΔgH-eGFP does not infect epithelial, endothelial, or fibroblasts, but infection of B cell remains equivocal. (a) Indicated cell types were seeded ($5x10^4$/well) in 48-well plates in triplicate and incubated with purified viruses (10^2 to 10^4 viral genome copies per cell) obtained from induced iSLK rKSHV WT-eGFP, iSLK rKSHVΔgH-eGFP, or iSLK rKSHVgH-eGFP Rev cells. After 48 h, eGFP+ cells were analyzed using flow cytometry (left) and imaged using EVOS Cell Imaging fluorescent microscopy (right) to determine viral infectivity. Representative flow cytometry plots and micrographs are shown (n≥3 independent experiments). **(b–d)** Tonsil-derived primary fibroblasts from four donors or MC116 cells were infected by spinoculation at 1500 x g for 1 h at RT with rKSHV WT-eGFP, rKSHVΔgH-eGFP, or rKSHVgH-eGFP Rev. Mock viral infection was performed using purified iSLK rKSHV WT-eGFP inactivated in 2% buffered formaldehyde in PBS for 60 min at 37°C. At Day 2 or 6 post-infection (dpi), tonsil-derived fibroblast cells or MC116 were analyzed; viable cells were gated from single cell populations, and eGFP+ cells were gated from viable cell populations. Tonsil-derived primary fibroblast cells (**b**) were not susceptible to infection by rKSHVΔgH-eGFP, whereas limited infection of MC116 B cells by rKSHVΔgH-eGFP (**c–d**) was observed. MC116 cells infected with viruses was imaged using EVOS Cell Imaging fluorescent microscopy. **(e)** (top panel). Percent infection of MC116 cells with formaldehyde-inactivated rKSHV WT-eGFP (mock), rKSHV WT-eGFP, rKSHVΔgH-eGFP, or rKSHVgH-eGFP Rev from three replicates (bottom panel) MC116 cells infected with formaldehyde-inactivated rKSHV WT-eGFP (mock), rKSHV WT-eGFP, or rKSHVΔgH-eGFP were FACS-sorted to enrich for eGFP expression. Sorted cells were grown for 4 days, lysed, and separated on 4-12% SDS-PAGE gels, then analyzed by immunoblotting for the expression of KSHV latent (LANA1) and lytic (K8.1) genes along with cellular housekeeping gene β-actin as control. **(f)** RT-qPCR confirmation of LANA1 and K8.1 gene expression. cDNA was synthesized from 100 ng total RNA extracted from MC116 cells infected with formaldehyde-inactivated rKSHV WT-eGFP (mock), rKSHV WT-eGFP, or rKSHVΔgH-eGFP (FACS-sorted and enriched for eGFP expression). Three μl of the resulting cDNA was used for RT-qPCR with KSHV LANA1 and K8.1 gene-specific primers and rKSHV WT-eGFP DNA was used as the standard for

quantification. RNA extracted from induced iSLK rKSHV WT-eGFP served as a positive control. Average Ct values obtained using GAPDH primers in individual samples are indicated below the graph. Samples were analyzed in triplicate and the experiment was repeated three times. (**g**) Immunoblot analysis of known gH/gL cellular receptors mediating KSHV infection in permissive human cells tested for infection. $1x10^6$ cells from each cell type were lysed and separated on 4-12% SDS-PAGE gels, then analyzed by immunoblotting using specific monoclonal antibodies against EphA2 (top), EphA4 (middle), or actin (bottom, loading control). **(h)** Flow cytometry analysis of EphA7 receptor expression in MC116, HEK-293 and iSLK cells.

FIG. 6. Non-human epithelial and fibroblasts cell lines are not permissive to rKSHVΔgH-eGFP infection. Indicated cell types were seeded ($5x10^4$/well) in 48-well plates in triplicate and incubated with purified viruses (10^4 viral genome copies per cell) obtained from induced iSLK rKSHV WT-eGFP, iSLK rKSHVΔgH-eGFP, or iSLK rKSHVgH-eGFP Rev cells. After 48 h, eGFP+ cells were analyzed using flow cytometry (left panels) and imaged using EVOS Cell Imaging fluorescent microscopy (right panels) to determine viral infectivity. Representative flow cytometry plots and micrographs are shown (n≥3 independent experiments).

FIG. 7. rKSHVΔgH-eGFP binding to target cells is not impaired. Attachment of KSHV to epithelial, endothelial, fibroblast, or B cells is not affected by absence of gH on KSHV virions. Cells were incubated with cold virus at the indicated concentrations at 4°C for 30 min, followed by DNA isolation. Quantification of the ratio of viral to cellular DNA as a measurement for attached virus was calculated based on ΔCt values of a viral locus (K8.1) and a genomic locus (GAPDH), as determined by qPCR and plotted against input viral genome number. Dashed grey (rKSHV WT-eGFP)/black (rKSHVΔgH-eGFP) lines show means of n≥3 independent experiments; error bars indicate standard deviation.

Table 1. List of primers used in mutagenesis and qPCR

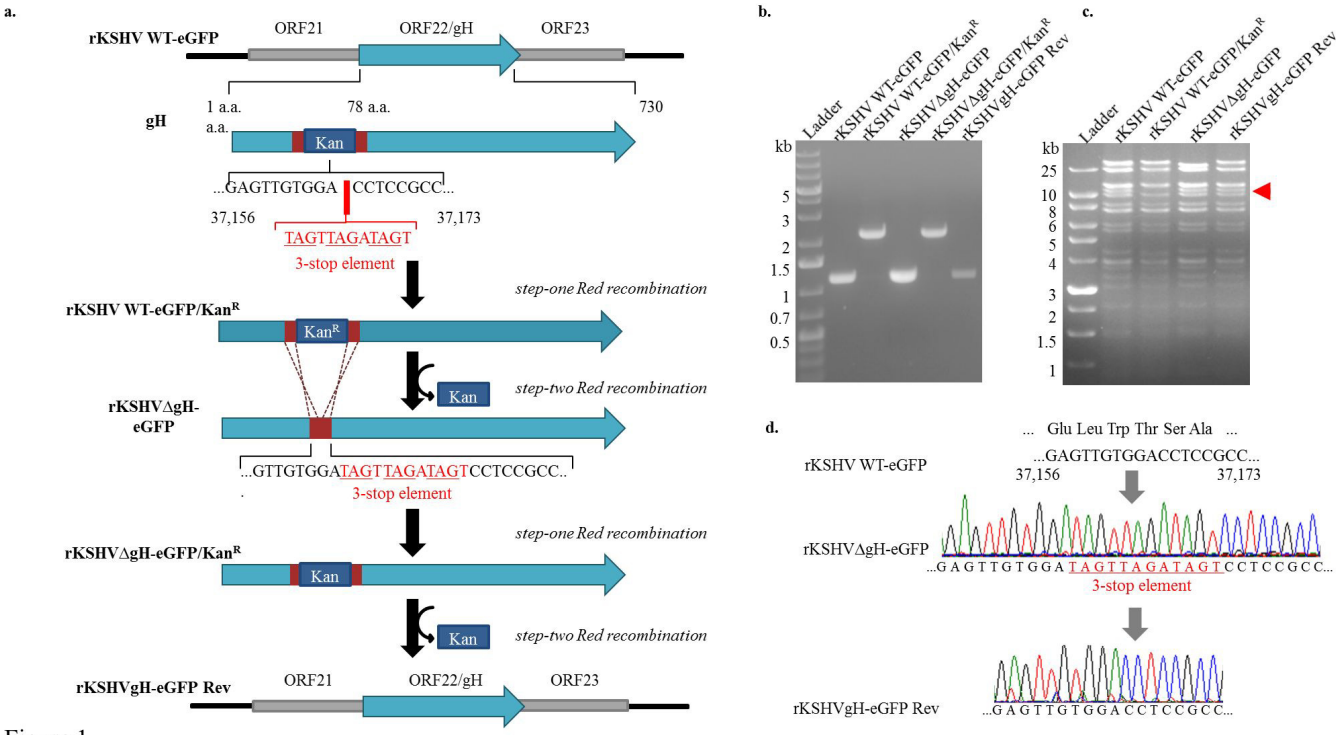

Figure 1

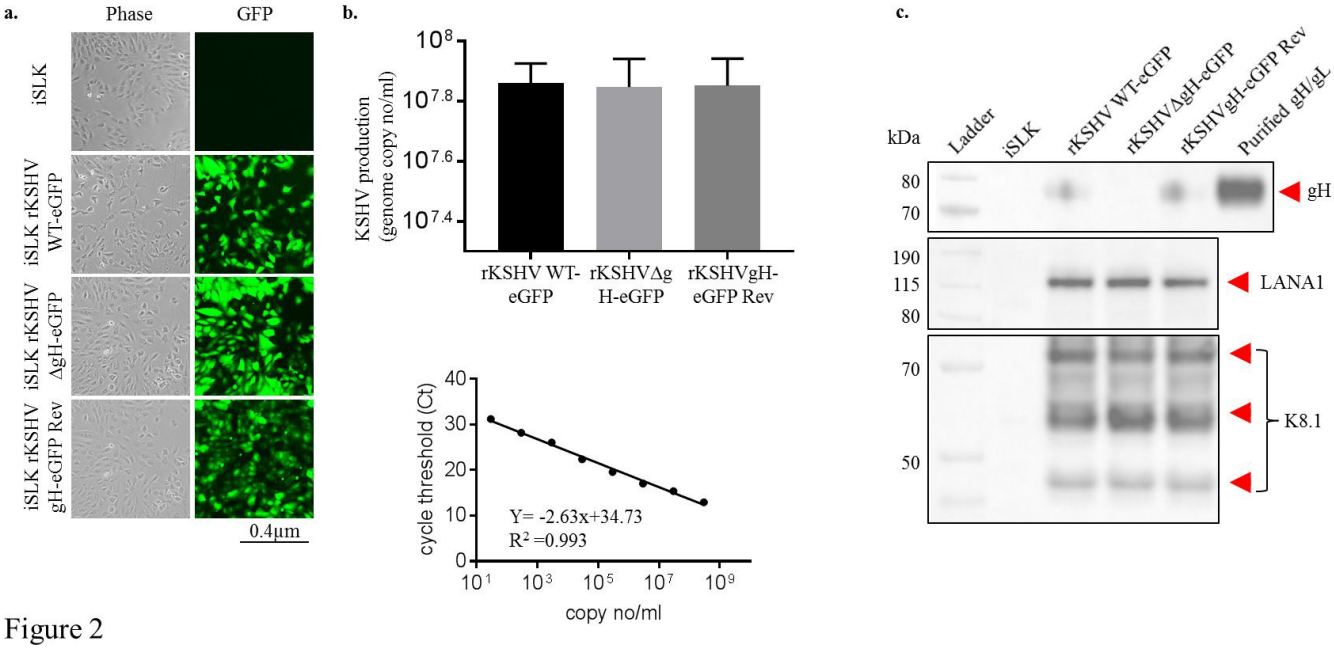

Figure 2

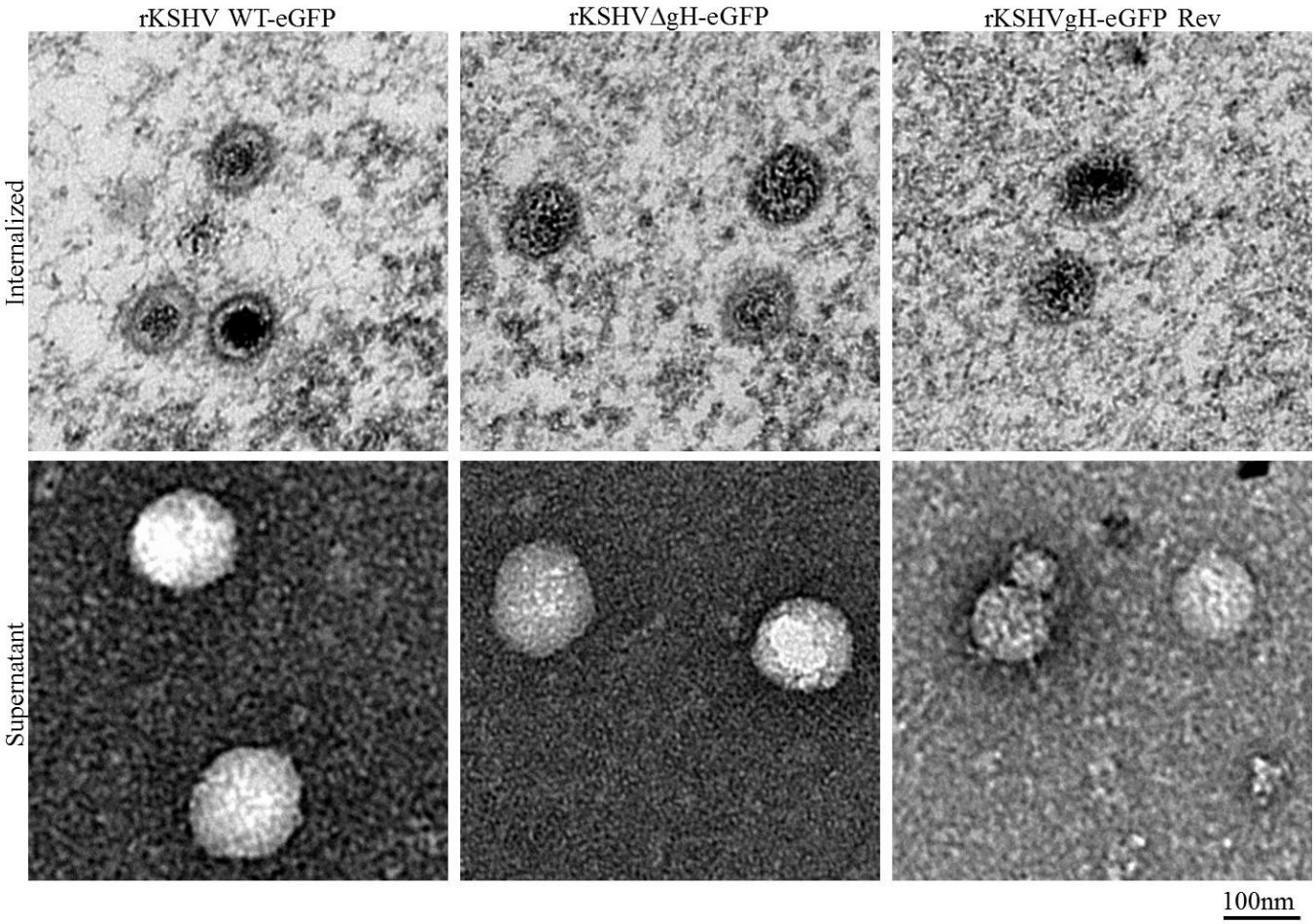

Figure 3

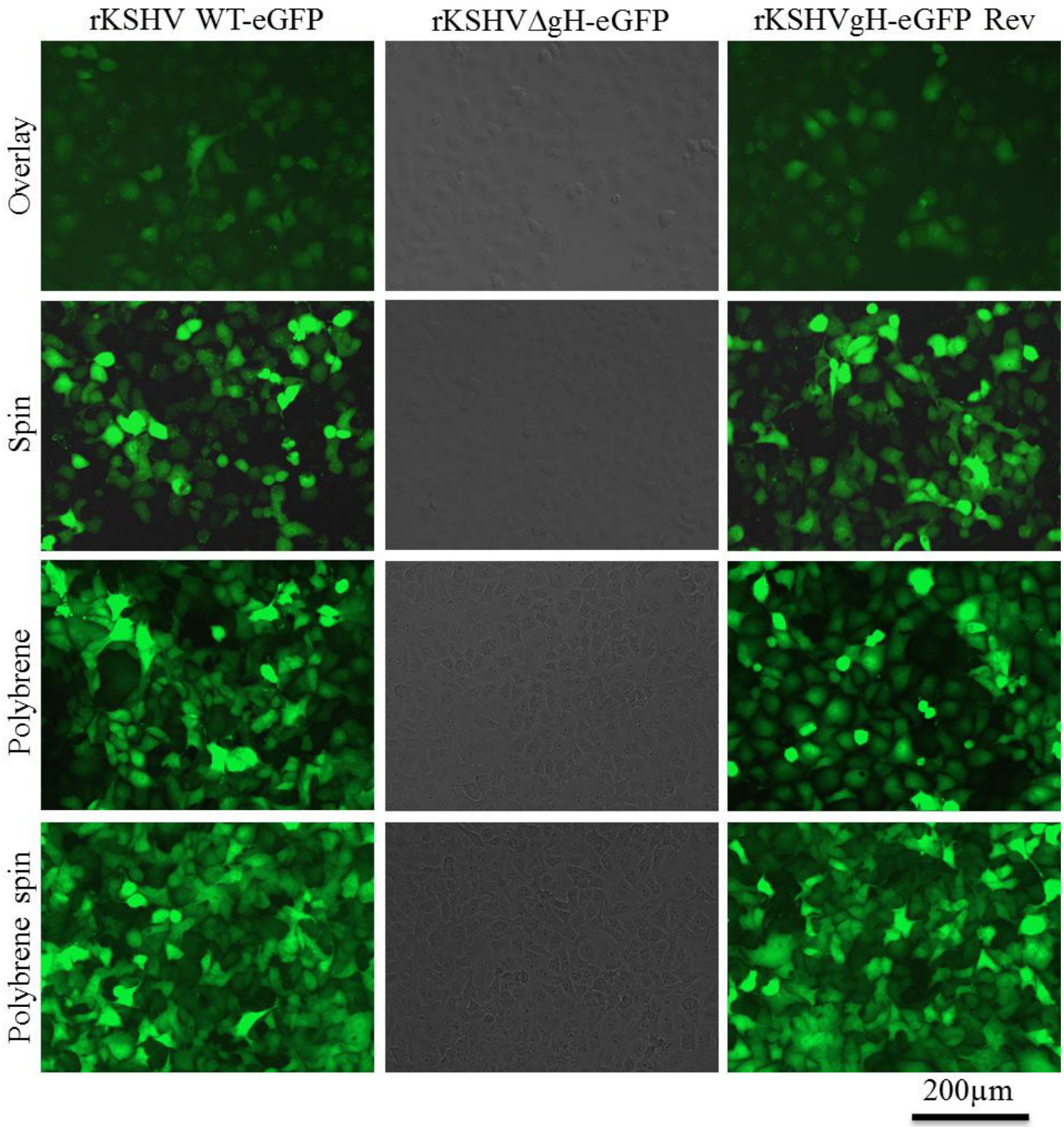

Figure 4

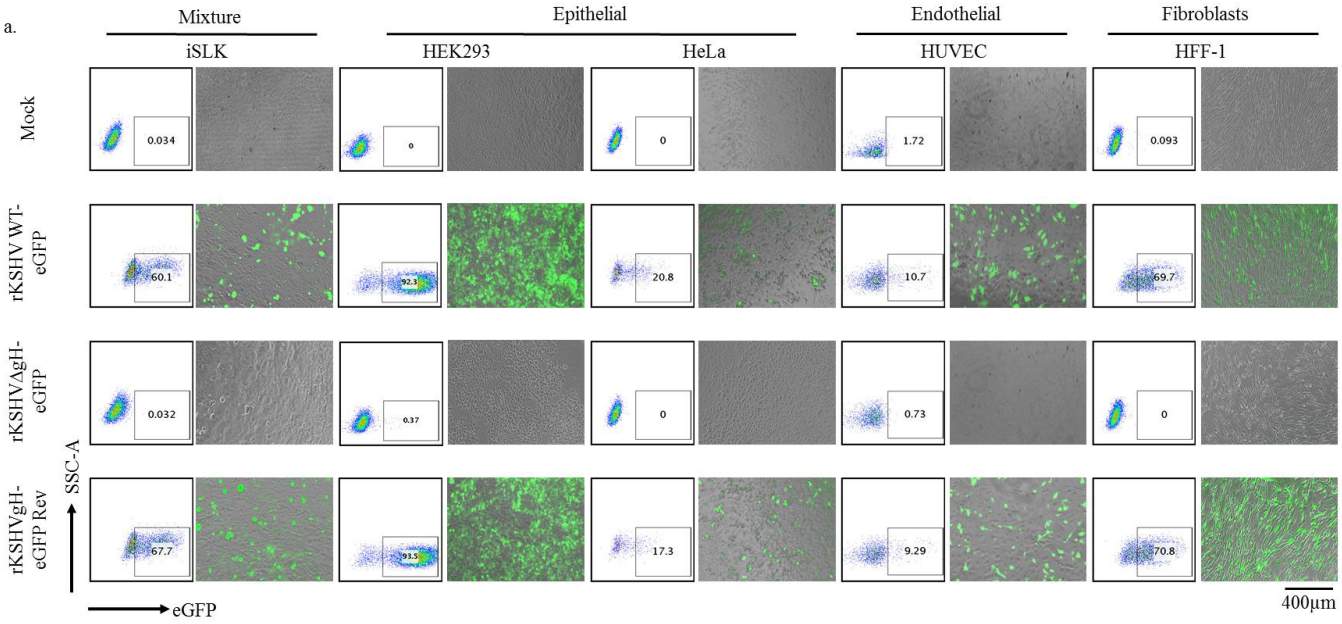

Figure 5a

Figure 5b-c

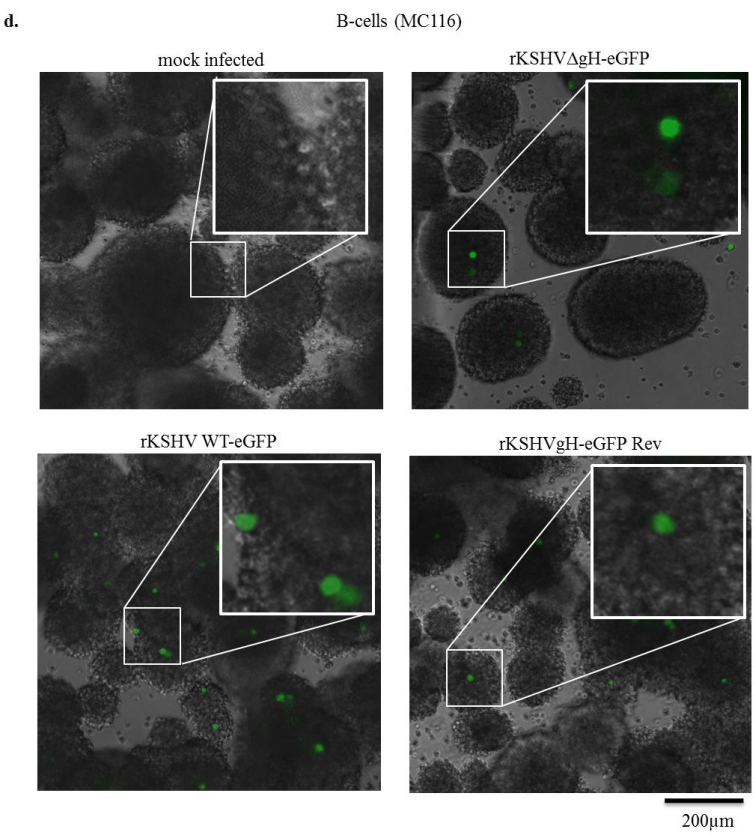

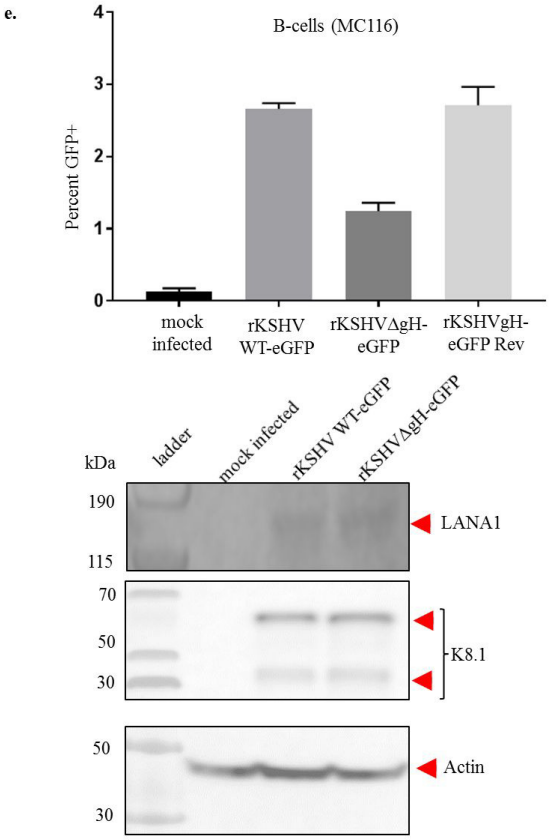

Figure 5d-e

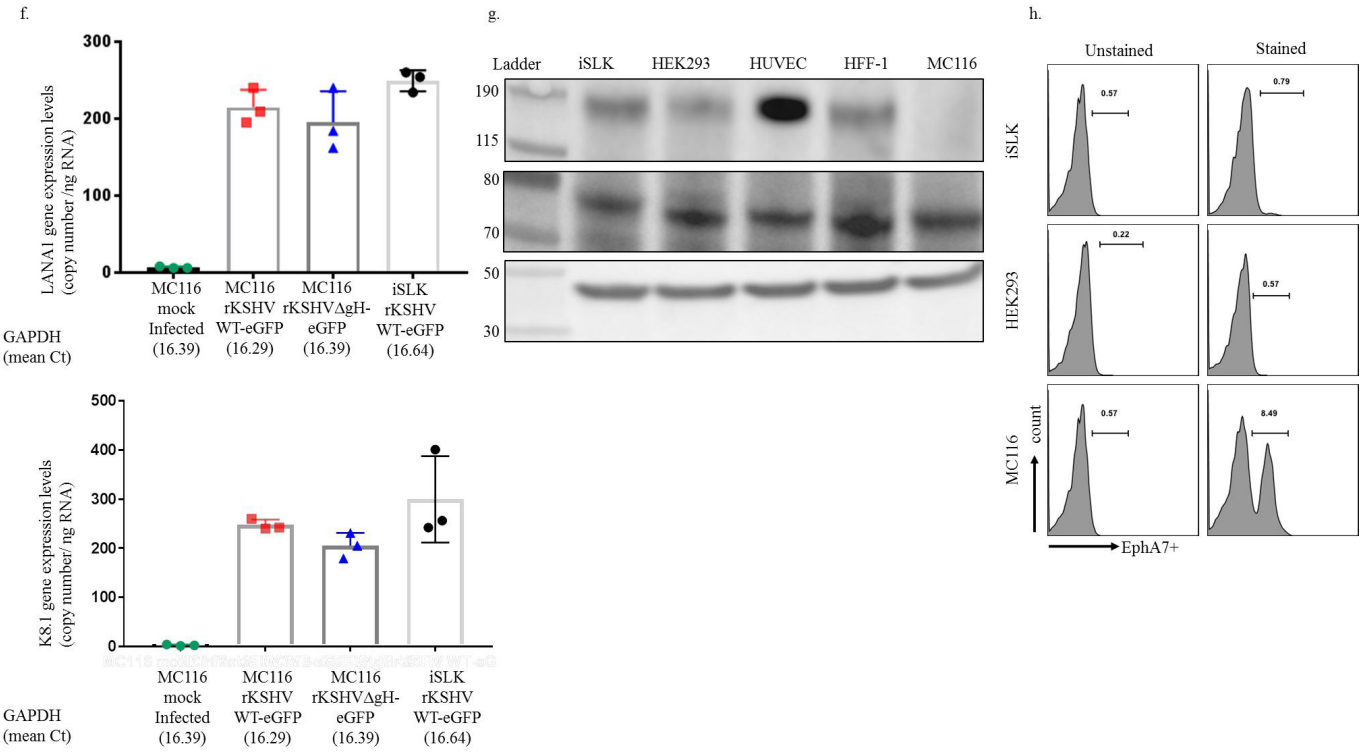

Figure 5f-h

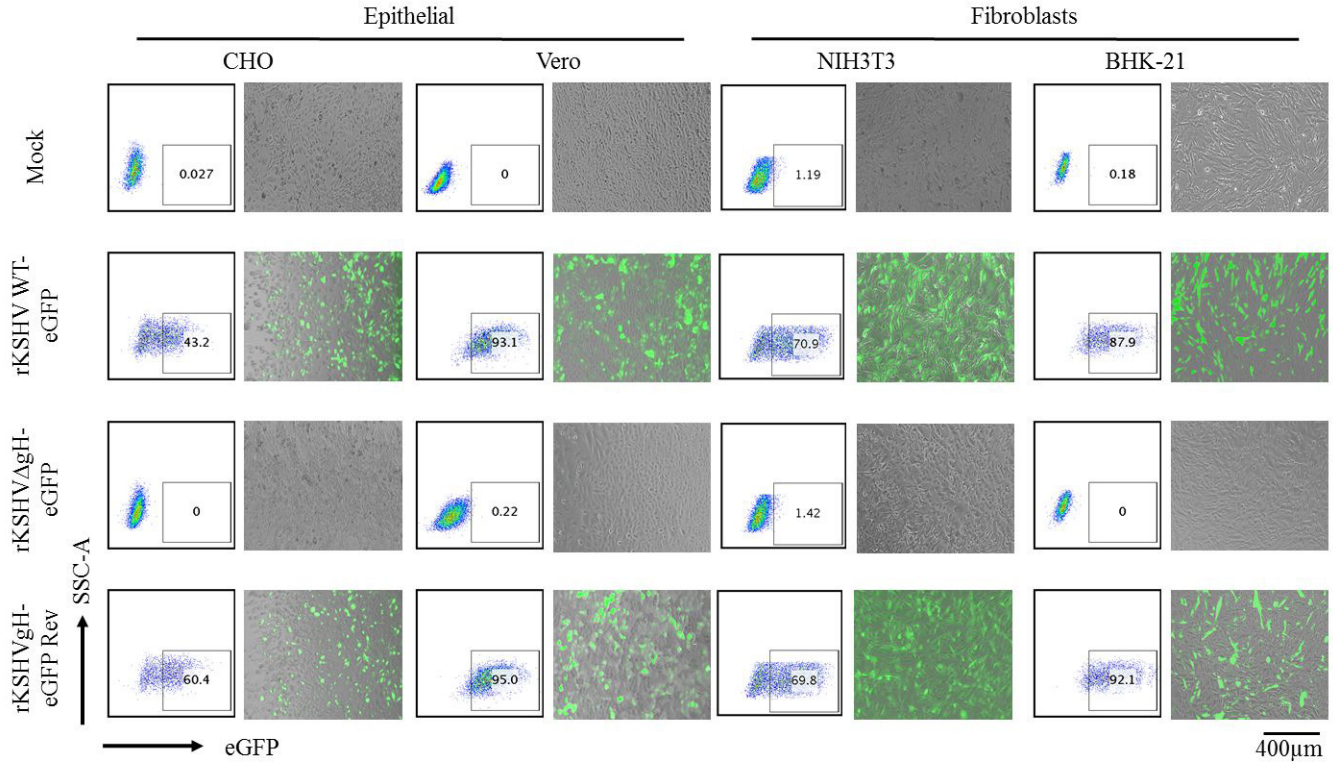

Figure 6

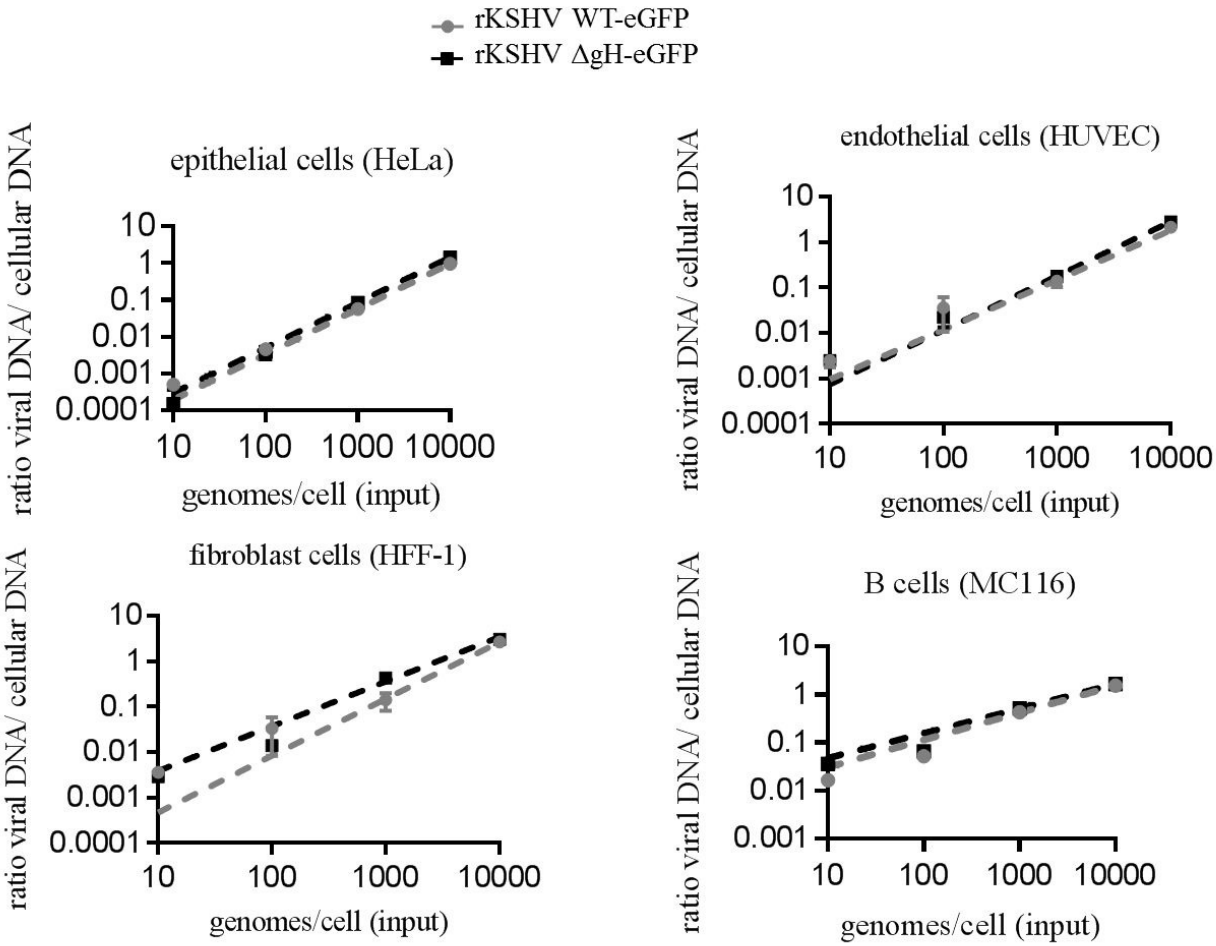

Figure 7

Primer type	Primer name	Primer sequence (5'-> 3')
BAC mutagenesis	BACmut-ORF22-3stop-F	ttgaatgtgatcacggagccggccctgacagagttgtggatAGTTAGATAGTcctccgccgaagtcgccgagTAGGGATAACAGGGTAATCGATTT
	BACmut-ORF22-3stop-R	ttcagagttaccctgaggtcctcggcgacttcggcggaggACTATCTAACTAtccacaactctgtcagggccGCCAGTGTTACAACCAATTAACC
	BACmut-ORF22-Rev-F	ttgaatgtgatcacggagccggccctgacagagttgtggatcctccgccgaagtcgccgagTAGGGATAACAGGGTAATCGATTT
	BACmut-ORF22-Rev-R	ttcagagttaccctgaggtcctcggcgacttcggcggaggtccacaactctgtcagggccGCCAGTGTTACAACCAATTAACC * Sequence homology; lowercase indicates to rKSHV WT-eGFP, underlined uppercase indicates three-stop codons mutagenesis site, and uppercase indicates pEP-KanR sequence
Gene specific	KSHV.219-ORF22-F	CTGGCGATGCATATCGTTG
	KSHV.219-ORF22-R	TGTTATAAGTTTGCGACGACG
	pEP-Kan F	ATGAGCCATATTCAACGG
	pEP-Kan R	CTCATCGAGCATCAAATG
qPCR	K8.1-F	TGCTAGTAACCGTGTGCCAT
	K8.1-R	AGATGGGTCCGTATTTCTGC
	LANA1-F	GCCTATACCAGGAAGTCCCA
	LANA1-R	GAGCCACCGGTAAAGTAGGA
	GAPDH-F	TGTCGCTGTTGAAGTCAGAGG
	GAPDH-R	CATCAAGAAGGTGGTGAAGCAG

Table. 1 List of primers used in mutagenesis and qPCR